AD-A048 294 ROYAL AIRCRAFT ESTABLISHMENT FARNBOROUGH (ENGLAND) F/G 4/1
VARIATIONS IN AIR DENSITY FROM JANUARY 1972 TO APRIL 1975 AT HE--ETC(U)
JUN 77 D M WALKER

UNCLASSIFIED RAE-TR-77078 DRIC-BR-58838 NL

1 OF 1
ADA048294

END
DATE FILMED
2-78
DDC

(19) BR-58838
(14) RAE-TR-77078

(8) DRIC

TR77078

ROYAL AIRCRAFT ESTABLISHMENT

*

(9) Technical Report 77078

(11) JUNE 77

(12) 43 p.

(6)

VARIATIONS IN AIR DENSITY FROM JANUARY 1972 TO APRIL 1975 AT HEIGHTS NEAR 200 km.

by

(10) Doreen M.C. Walker

*

Procurement Executive, Ministry of Defence
Farnborough, Hants

310 450

UDC 551.501.71 : 551.510 535

ROYAL AIRCRAFT ESTABLISHMENT

Technical Report 77078

Received for printing 2 June 1977

VARIATIONS IN AIR DENSITY FROM JANUARY 1972 TO APRIL 1975 AT HEIGHTS NEAR 200 km

by

Doreen M. C. Walker

SUMMARY

Variations in air density have been determined using the orbit of satellite Cosmos 462, 1971-106A, which entered orbit on 3 December 1971 with an initial perigee near 230 km and inclination 65.75°, and decayed on 4 April 1975. Accurate orbits determined at 85 epochs give perigee height correct to about 200 m throughout the satellite's lifetime. Using these values of perigee height and orbital decay rates from NORAD elements, 604 values of air density at half a scale height above perigee have been evaluated. These densities have been compared with values from the COSPAR International Reference Atmosphere 1972, taking account of variations due to solar activity and geomagnetic disturbances, and day-to-night variations, to reveal the residual variations in density at a series of standard heights, 245, 240, 232 and 213 km.

The main residual variation is semi-annual, with maxima usually in April and October, and minima usually in January and July; but it is irregular in phase and shape. The amplitude of the semi-annual variation is remarkably constant from year to year between 1972 and 1975, and considerably greater than that given by *CIRA 1972*: the April/July density ratio is 1.68, not 1.32 as in *CIRA*; the October-November maxima are all lower than the April maxima, whereas *CIRA* gives the opposite; the July minima are 18% lower than the January minima, as opposed to 10% in *CIRA*.

A standardized semi-annual density variation for the early 1970s is presented, with January minimum of 0.94, April maximum of 1.28, July minimum of 0.77 and October-November maximum of 1.22. In addition, three other recurrent variations are recognizable: in each year the density has a subsidiary minimum in May and maximum in June; there are low values in mid November and high values in late December.

Departmental Reference: Space 528

LIST OF CONTENTS

1 INTRODUCTION

The density of the upper atmosphere at heights between 150 and 1000 km has been studied quite thoroughly from the analysis of satellite orbits, and the results of these studies prior to 1972 have been incorporated in the COSPAR International Reference Atmosphere 1972[1]. The main changes in density are due to the effects of solar extreme ultraviolet radiation, the day-to-night variation, geomagnetic activity and the semi-annual variation. Values of density obtained from orbital decay rates of satellites can be cleared of the first three effects with the aid of *CIRA 1972*, by utilizing the indices of solar activity and geomagnetic disturbance in retrospect. Removal of these effects exposes the residual variations, a mainly semi-annual variation with maxima usually in April and October and minima usually in January and July. The semi-annual variation, first detected[2] in 1961, has been followed until early 1972 by analysing various satellite orbits[3-8]. The aim of this Report is to evaluate the density at heights near 200 km and trace the semi-annual variation from January 1972 to April 1975 using the satellite Cosmos 462.

Cosmos 462 was launched on 3 December 1971 and was one of a pair of satellites launched by the Russians to test high-speed interception[9,10]. Cosmos 462 was the hunter satellite and exploded after passing the target satellite, Cosmos 459. This explosion occurred 3.5 hours after launch and the largest piece of the satellite remaining in orbit was designated 1971-106A.

After this experiment, 1971-106A had an orbital period of about 105 minutes, perigee height 230 km, apogee height 1800 km and inclination, i, 65.7°; the satellite remained in orbit for 40 months, without further disturbance, and decayed naturally on 1975 April 4.90[11].

During its lifetime 1971-106A was selected for high-priority observing by the British optical and radar tracking stations, including the Hewitt cameras at Malvern and Edinburgh. Observations were also available from the United States Navy, kindly supplied by the US Naval Research Laboratory; from the Cape kinetheodolite at the South African Astronomical Observatory; and the theodolite at Jo[illegible]en, Finland. Using some 5400 observations, accurate orbits at 85 epochs have been computed at RAE[12] throughout the satellite's life.

The perigee heights obtained at the 85 epochs have been used, together with the orbital decay rates calculated from NORAD elements, to derive 604 values of air density at heights between 176 and 252 km.

2 ORBITAL DECAY RATE

The orbital decay rate, $\dot{n}$, was found with adequate accuracy from the NORAD elements at an average interval of two days. The values of the mean anomalistic motion n (rev/day) were differenced to give values of Δn, each of which was divided by the corresponding time interval Δt (day) to give values of $\dot{n} = \Delta n/\Delta t$ (rev/day^2). Any erroneous value of n causes an up-down pattern in $\dot{n}$, *ie* one value too high the next too low, or vice versa. After inspecting the values of $\dot{n}$, 57 values of n responsible for up-down patterns were eliminated; the remaining 604 values of $\dot{n}$ are plotted as circles in Figs 1 and 2. The values of $\dot{n}$ from the 85 RAE orbits are plotted as triangles. The two sets of values show excellent agreement, especially when it is remembered that the RAE values are for specific dates and the values from NORAD elements are averaged over a time interval Δt.

The effects of solar radiation pressure on $\dot{n}$ are negligible: they are calculated to be less than 0.02% of the main effects due to air drag.

3 PERIGEE HEIGHT

3.1 Variation of perigee distance, $a(1 - e)$

Fig 3 shows values of perigee distance $a(1 - e)$, plotted as circles, from the 85 orbits[12] determined at epochs spread quite evenly over the satellite's 40-month life, where a is the semi major axis and e is the eccentricity. For most satellites, $a(1 - e)$ suffers a regular oscillation, of amplitude several kilometres and period a few months, caused by the effects of the odd zonal harmonics in the Earth's gravitational potential, and also small oscillations due to lunisolar perturbations. Some smoothing of the observational values of $a(1 - e)$ is required and in the past[7] this has been done by clearing the odd-zonal harmonic oscillation from $a(1 - e)$ to give corrected values, which should show a steady slow decrease as a result of air drag (apart from small oscillations due to lunisolar perturbations). A smooth curve was then drawn through the corrected values and the odd-zonal harmonic perturbation restored to give smoothed values of $a(1 - e)$. The satellite 1971-106A has an orbital inclination (65.7°) at which the oscillation due to odd-zonal harmonics is unusually small[13], its amplitude being about 1.5 km, and the period is unusually long, about two years. Consequently the values of $a(1 - e)$ show only a small and slow variation, and a smooth curve could be drawn through the points plotted as circles. However, as the odd-zonal harmonic oscillation is so small, the oscillation due to lunisolar perturbations is of the same order, so better

accuracy can still be achieved by calculating the zonal-harmonic and lunisolar perturbations, removing these perturbations, and drawing a smooth curve through the corrected values of $a(1 - e)$, Q say. The perturbations due to zonal harmonics and lunisolar effects have been calculated by numerical integration at one-day intervals using the PROD computer program[14]. The values of Q, which should now show a steady decrease as a result of air drag alone, are plotted as crosses in Fig 3 and a smooth curve has been drawn through the points. All the values have standard deviations of 0.2 km or less.

3.2 Perigee height, y_p

The actual perigee height, y_p, above the Earth's surface is found by first restoring the zonal-harmonic and lunisolar perturbation to the smoothed values of Q, giving smoothed values of perigee distance, $a(1 - e)_{\text{smoothed}}$; then from these values subtracting the local Earth's radius, R_p, at latitude ϕ_p given by

$$R_p = R - 21.38 \sin^2\phi_p \qquad (1)$$

where R is the Earth's equatorial radius, 6378.14 km; and finally adding the small amount by which the actual path of the satellite departs from an exact ellipse[15], dr_p, where, with error less than 20 m, we may write

$$dr_p = 1.388 \left[1 - \frac{2}{1+e}\sin^2\omega\right] \quad \text{km} \qquad (2)$$

where ω is the argument of perigee. Thus, since $\sin^2\phi_p = \sin^2 i \sin^2\omega$, the values of perigee height are given by

$$y_p = a(1 - e)_{\text{smoothed}} - 6378.14 + 21.38 \sin^2 i \sin^2\omega + 1.388 \left[1 - \frac{2}{1+e}\sin^2\omega\right]$$

$$= a(1 - e)_{\text{smoothed}} - 6376.75 + \left(17.76 - \frac{2.78}{1+e}\right)\sin^2\omega \quad . \qquad (3)$$

The values of y_p calculated at the 85 epochs using equation (3) are plotted as circles in Fig 4 and a smooth curve has been drawn through the points.

4 EVALUATION OF AIR DENSITY

4.1 Determination of density

The air density ρ_A at a height $\frac{1}{2}H^*$ above perigee was obtained from $\dot{n}$ by using the equation[16]

$$\rho_A = \frac{0.157(1000\dot{n})}{10^6 n^2 \delta}\left(\frac{e}{aH^*}\right)^{\frac{1}{2}} \frac{(1-e)^{\frac{1}{2}}}{(1+e)^{\frac{3}{2}}}\left\{1 - \frac{H^*}{8ae}\left(1 - 8e + \frac{7H^*}{16ae}\right) + \frac{\varepsilon \sin^2 i \cos 2\omega}{e}\right\} \qquad (4)$$

where ε is the ellipticity of the atmosphere (taken as 0.00335) and δ is an area/mass parameter[16].

This equation was originally derived[17] with the aim of minimizing errors in ρ_A due to errors in knowledge of scale height: H* was defined as the 'best estimate' of the value of the density scale height H at perigee, and the equation was designed to allow errors of up to 25% in H* without incurring an error of more than 1.2% in ρ_A. Although it is now possible to assign much more accurate values to H* (correct to perhaps 5%), it is still convenient to take advantage of the insensitivity of ρ_A to errors in H* by computing density using a constant value of H* over time intervals during which H does not vary by more than about 10% as a result of changes in perigee height and solar activity. For 1971-106A, suitable time intervals are 12, 12, 9 and 5½ months. During the first of these chosen time intervals the variations in the current value of H are assessed as about 6% (sd) due to variations from day to night and variations with solar activity, and about 4% (sd) due to the changes in perigee height (±6 km). Thus the total error in H* is estimated as 7% (sd), giving an error of about 0.5% (sd) in ρ_A. The other three intervals have nearly the same standard deviations in ρ_A.

The constant coefficient, 0.157, outside the brackets in equation (4) is also a function of the gradient of scale height μ (= dH/dy), and the numerical value 0.157 was obtained[16] on the assumption that $\mu = 0.1$. For 1971-106A the appropriate values of μ are (from *CIRA 1972*) between 0.13 and 0.18, and the departure of μ from its assumed value of 0.1 creates an error, estimated[17] as 1.3% (sd), in the coefficient 0.157. However this error in the formula (4) is automatically cancelled by the method of determining δ (see below) and need not be considered. Further errors in equation (4) are caused by the neglect of small terms in the expansion, which are of order e^4, $\frac{1}{4}c^2 \cos 4\omega$, $\frac{1}{8}\mu^2$, etc[16], where $c = (\frac{1}{2}\varepsilon r_p \sin^2 i)/H$. For 1971-106A the largest of these terms is $\frac{1}{4}c^2 \cos 4\omega$, which has a mean value of 0.010. Thus there are two relevant error terms in equation (4), 0.5% from variation in H, and 1.0% from neglected terms, leading to a total error in ρ_A of 1.1% (sd) for given values of $\dot{n}$ and δ.

The values of H were taken from *CIRA 1972*, which gives the variation of H with height for different exospheric temperatures. Equation (4) is valid if $3H^*/a < e < 0.2$; these conditions are satisfied until three weeks before decay.

After 13 March 1975, when $e < 3H^*/a$, the density was evaluated using the equation[16]

$$\rho_\lambda = \frac{1000\dot{n}\Phi}{3\pi a\delta n^2 \times 10^6} \left\{ \frac{\exp(c \cos 2\omega)}{1 + 2eI_1(z^*)/I_0(z^*) + cI_2(z^*)/I_0(z^*) \cos 2\omega + c^2/4} \right\} \quad (5)$$

where $z^* = ae/H^*$, $I_n(z^*)$ is the Bessel function of first kind and imaginary argument of order n and Φ is given by Fig 7.4 of Ref 16. The values of density from both equation (4) and equation (5) are obtained in kg/m^3 if H^* and a are in km, the area/mass parameter δ is in m^2/kg, n is in rev/day and $\dot{n}$ in rev/day^2.

The values of air density ρ_A from equation (4) are at a height $y_A = y_p + \frac{1}{2}H^*$, and the values ρ_λ from equation (5) are at a height $y_\lambda = y_p + \lambda H^*$. The value of λ is 0.5 when $ae/H^* \geqslant 1$ and this condition is satisfied for all the values of ρ_λ calculated. So, throughout the life of the satellite the density is evaluated at a height $y_A = y_p + \frac{1}{2}H^*$.

The value of the area/mass parameter δ for 1971-106A is not known and was chosen to give values of density in conformity with *CIRA 1972*. First, the density during 1972 was calculated from equation (4) taking a nominal value of 0.01 for δ; then the density for the appropriate local time, solar activity, etc, as given by *CIRA*, was evaluated at six dates in 1972 when the semi-annual variation was near its mean value (February, May, September). The values of δ needed to bring the values of density from equation (4) into agreement with those from *CIRA* were 0.0069, 0.0074, 0.0072, 0.0080, 0.0069 and 0.0080 m^2/kg, giving an average δ of 0.0074 with rms error 6%.

4.2 Conversion to standard height

In order to examine day-to-day variations in density it is necessary to convert the values of density to a fixed height y_B, say, which may most appropriately be taken as the mean value of y_A over the same time intervals as those used in section 4.1 for H^* when calculating density ρ_A. The density ρ_B at height y_B is calculated from the equation

$$\rho_B = \rho_A \exp\left(\frac{y_A - y_B}{H_B}\right) \quad (6)$$

where H_B is the value of H at height y_B. Since the value of H_B may be in error by about 7% (sd) due to day-to-day variations in H, and the rms values of $(y_A - y_B)$ for each of the four time intervals are 4.7, 5.3, 3.7 and 4.4 km respectively, the total errors in ρ_B due to the use of equation (6) will be 1.4%, 1.6%, 1.4% and 1.6% respectively. The actual time intervals taken and the values of the various parameters are given in Table 1.

Table 1

Four time intervals and values of parameters

Time interval MJD	Mean y_p km	H* km	y_B = mean y_A km	H_B km
41317 - 41682 (1972)	227	36	245	39
41683 - 42047 (1973)	223	34	240	37
42048 - 42320 (1 Jan - 30 Sep 1974)	216	32	232	35
42321 - 42483 (1 Oct 1974 - 12 Mar 1975)	198	30	213	32

Between the end of the fourth interval (13 March 1975) and decay (4 April 1975) the perigee height decreases rapidly and conversion of ρ_λ to a fixed height is no longer advantageous.

5 PRESENTATION AND ANALYSIS OF DENSITY

5.1 Variation of density with time

The values of density, ρ_B, obtained at fixed heights y_B for each of the four time intervals - ρ_{245}, ρ_{240}, ρ_{232} and ρ_{213} - are plotted as circles joined by lines at the top of Figs 5, 6, 7 and 8 respectively. The values of ρ_λ near decay are shown in similar format in Fig 9. The three curves below the density values in Figs 5 to 9, in descending order, are: (1) solar radiation energy on 10.7 cm wavelength, $F_{10.7}$, as measured by NRC, Ottawa; (2) sun-perigee angle, with the local time at perigee in hours marked above the curve and the latitude of perigee in degrees marked below the curve; and (3) the daily planetary geomagnetic index, Ap, as given by the Institut für Geophysik, Göttingen, plotted with a 12-hour time lag.

5.2 Comparison with *CIRA 1972* model

From *CIRA 1972*, values of density can be obtained for the same times as the densities evaluated from the orbital decay rates. The *CIRA* model gives tables of density against height for a range of exospheric temperatures. To obtain the values of density on a particular day, the exospheric temperature has to be evaluated for the appropriate conditions of (a) solar activity, (b) local time at perigee, latitude of perigee and solar declination, and (c) geomagnetic disturbance. By comparing ρ_B with the corresponding value

from *CIRA*, the residual density variations (including the semi-annual variation) can be traced. Seasonal-latitudinal variations in helium have no effect because the proportion of helium is negligible at heights near 250 km.

5.2.1 Variation with solar activity

The upper-atmosphere temperature and density reflect changes in solar activity, on daily, monthly and 11-yearly time scales, and the 10.7cm solar flux, $F_{10.7}$, is generally used as the best available index of solar EUV radiation. In order to evaluate density from the *CIRA* model at a particular height, the night-time minimum temperature, T_c, in kelvins, is computed from equation (14) in Part 3 of *CIRA*

$$T_c = 379 + 1.94 \bar{F}_{10.7} + 1.3 F_{10.7} \qquad (7)$$

where $\bar{F}_{10.7}$ is the mean flux averaged over six solar rotations (centred on the current date) and $F_{10.7}$ is the flux over the time that the density is being determined (usually one to two days). The value of T_c applies for an undisturbed geomagnetic field (Kp = 0).

5.2.2 The day-to-night variation

At heights above about 200 km the density of the upper atmosphere undergoes a diurnal variation, with maximum density and temperature at about 14 h local time and minimum at about 3 h local time. To obtain local exospheric temperature for use on the *CIRA* model, the local solar time at perigee and latitude of perigee are evaluated at intervals of approximately 20 days, corresponding to 5^o changes in the Sun's declination; then the appropriate value of T_ℓ/T_c, the ratio of the local exospheric temperature at perigee T_ℓ, to the minimum night-time temperature T_c, is obtained from Table 1 in Part 3 of *CIRA*. These values of T_ℓ/T_c are plotted against time and a smooth curve is drawn through the points, Fig 10. Values of T_ℓ/T_c can then be read off the curve at the date of each density value. The values of T_ℓ thus obtained, using T_c from equation (7), are for an undisturbed geomagnetic field (Kp = 0), as with T_c.

5.2.3 Variations with geomagnetic activity

The Sun also affects the upper atmosphere on a day-to-day basis through the incoming particles of the solar wind. When the Sun erupts with flares, intense streams of charged particles are emitted which create geomagnetic storms. These can last for a few hours or a few days and cause large increases in density. The geomagnetic effect on the temperature in kelvins is given in *CIRA 1972* as

078

$$\Delta T = 28Kp + 0.03 \exp(Kp) \qquad (8)$$

in which Kp is the 3-hour geomagnetic planetary index. In this study, with density evaluated at average intervals of two days, the daily geomagnetic index Ap is more convenient to use and since the relationship between Ap and Kp is known[18], equation (8) gives ΔT as a function of Ap, and is shown in Fig 11. As Ap ranges from 2 to 400, ΔT varies from 9 to 500 kelvins. Values of ΔT are read from the curve of Fig 11 for values of Ap corresponding to the mean interval over which the density is being estimated. These values of ΔT are added to the values of T_ℓ to give the appropriate value of exospheric temperature, T_∞, corresponding to each of the 604 values of density evaluated from orbital decay.

5.2.4 Density index, D

Using the values of exospheric temperature, T_∞, corresponding densities can be obtained from Table 6 in Part 3 of *CIRA 1972*. These values of density, ρ_{CIRA}, are for the conditions of solar activity, diurnal variation and geomagnetic disturbance over the same time interval as the densities evaluated from the orbital decay rates.

To display the results, the values of density from the orbital decay, ρ_B, are divided by ρ_{CIRA} to give a 'density index', D, so that

$$D = \rho_B/\rho_{CIRA} \qquad (9)$$

for each of the four fixed heights, y_B, given in Table 1. The values of D for each of the four time intervals are plotted as circles and joined by straight lines at the bottom of Figs 5 to 8.

Between 13 March 1975 and decay (4 April 1975), where the values of density ρ_λ are not converted to a standard height, the values of D are given by ρ_λ/ρ_{CIRA} where ρ_{CIRA} is evaluated at height y_λ. Thus each value of D is for a different height, but still represents the ratio of the density from orbital decay to *CIRA* density. These values of D are plotted at the bottom of Fig 9. The values of y_λ are also plotted with ρ_λ at the top of Fig 9.

6 RESULTS

6.1 The semi-annual variation

The values of the density index, D, displayed at the bottom of Figs 5 to 9 give a record of the residual variations in density after removal of the main effects of solar activity, day-to-night variations in density, and geomagnetic disturbances. After these major disturbances due to the Sun have been accounted for, the most important remaining variation in density has a semi-annual recur-

rence tendency, generally following a pattern of maximum density in April and late October, and minimum in January and July.

In the results from 1971-106A the course of this semi-annual variation can be traced in the values of density index, D. The form of the semi-annual variation is most readily revealed by drawing two parallel curves through the jagged observational values, as in Figs 5 to 8, in such a way that the majority of the observational values are included in the band defined by the two curves, which is about 0.15 wide, that is approximately 15%. The maximum and minimum values in the semi-annual variation may then be taken as the maximum and minimum of a curve midway through the band. The values of D thus obtained, with the corresponding dates, are given in Table 2.

Table 2

Semi-annual maxima and minima in density index D

Year	Height y_B km	January-February minimum		March-April maximum		July-August minimum		October-November maximum	
		Date	D	Date	D	Date	D	Date	D
1972	245	Feb 20	0.95	Apr 19	1.30	Aug 2	0.81	Oct 30	1.23
1973	240	Jan 18	0.94	Apr 8	1.29	Jul 17	0.75	Nov 27	1.18
1974	232	Jan 18	0.91	Mar 18	1.27	Jul 20	0.74		
	213							Oct 30	1.26
1975	213	Feb 17	0.97						
Mean values		Feb 3	0.94	Apr 5	1.29	Jul 23	0.77	Nov 8	1.22
CIRA values		Jan 16	0.94	Apr 6	1.12	Jul 27	0.85	Oct 27	1.16

Several features of Table 2 and Figs 5 to 8 call for comment:

(1) There is only a small variation from year to year in the value of the density index at a particular maximum or minimum of the semi-annual variation: the mean values are within 5% of the individual values. Three of these mean values however differ significantly from those of *CIRA 1972*; the April and October maxima are 15% and 5% higher than in *CIRA* and the July minimum is 9% lower; the January minimum value is the same as in *CIRA*.

(2) The October maxima are all lower than the April maxima, the mean value being 5% lower. This does not conform with *CIRA*, where the October value is 4% higher than the April value. The *CIRA* model was based on values determined from satellite orbital analysis in the 1960s, when the October maximum was usually the higher[19]. The results for 1972-75 do however agree with values

determined from 1970-65D, where the 1970 November maximum was 4% lower than the 1971 April maximum[7]. The high April maxima may therefore be regarded as a phenomenon of the 1970s.

(3) As in *CIRA*, the July minimum is stronger than the January minimum, but for the years covered by this study the July minimum is 18% stronger, while *CIRA* gives it as only 10% stronger.

(4) The shape of the variation is not sinusoidal, and the maxima and minima are not at regular intervals. The most striking departure from a sinusoidal curve in all three years is the rapid rise to a short-lived maximum in April, followed by a long slow decline to the flat July-August minimum. The mean dates of the maxima and minima are given in Table 2 but the individual dates differ from the mean by as much as 19 days. The dates of the *CIRA* maxima and minima are also given in Table 2: the April maximum and July minimum agree to within 4 days, but the January minimum and October maximum differ by 18 and 12 days respectively. But it should be noted that although the mean date obtained for the April maximum agrees with the *CIRA* date (April 5) the individual dates differ: the maximum in 1974 occurred 18 days earlier, on March 18. This emphasizes how variable is the phase of the semi-annual variation.

The values of the ratios of the April maximum to the January and July minima, and the October maximum to the July and following January minima, are shown in Table 3. The values for each individual ratio for each of the three years are suprisingly constant by comparison with the 1960s when there was considerable variation from year to year. The factors of variation are, of course, considerably greater than those from *CIRA*, shown in the last column of Table 3.

Table 3

Ratio of semi-annual maximum/minimum for 1972-1974

	1972	72/73	1973	73/74	1974	74/75	Mean	*CIRA*
April maximum/ January minimum	1.37		1.37		1.40		1.38	1.19
April maximum/ July minimum	1.60		1.72		1.72		1.68	1.32
October maximum/ July minimum	1.52		1.57		1.70		1.60	1.36
October maximum/ January minimum		1.31		1.30		1.30	1.30	1.23

6.2 Other variations in density index, D

6.2.1 Day-to-day variations

The jaggedness of the density index in Figs 5 to 8 reveals how the density varies from day to day. The two parallel curves drawn to show the course of the semi-annual variation enclose most of the jagged observational values. So the change in density from day to day amounts to about ±7%.

There is very little likelihood that changes in cross-sectional area contribute to the jaggedness. A satellite that rotates many times while in the region near perigee where drag is important (a region which takes about 10 minutes to traverse) will have an effectively constant cross-sectional area, the average over a rotation. The flash period of 1971-106A increased from about 4 seconds just after launch to about 20 seconds early in 1973, with no abrupt changes; during 1972, therefore, the satellite rotated many times in the region near perigee, on each orbit. So the jaggedness in 1972 cannot be caused by variations in cross-sectional area, and since the appearance of the graphs for 1973-75 is very similar, there is no reason to suspect irregular variations in cross-sectional area during 1973-5.

6.2.2 Effect of geomagnetic storms

The observational values of density plotted at the tops of Figs 5 to 8 show correlation with geomagnetic activity. The density index D gives the values after removal of these effects (see section 5.2.3) using Jacchia's equation for ΔT in *CIRA 1972*, equation (8). However, it can be seen that on some occasions the effect has not been fully removed. This may be because the geomagnetic index used, Ap, does not always indicate the full effect of a magnetic storm on the upper atmosphere, partly because of the incomplete geographical distribution of magnetic observatories whose data are used in the production of the indices[20], and partly because these measurements of effects at ground level may not adequately reflect the effects on the upper atmosphere. This could very well be the case at MJD 41438, where there is a sudden increase in density but only a relatively small magnetic storm is indicated by the Ap index (Ap = 40). A similar increase occurred at MJD 42280 and again the Ap index was small.

It may be that the geomagnetic effect could be more adequately removed by
078 representing the geomagnetic variations by a latitude-dependent approximation, such as that given by Roemer[21],

$$\Delta T = (21.4 \sin |\phi| + 17.9)\bar{K}p + 0.03 \exp \bar{K}p \quad \text{kelvins} \qquad (10)$$

where $\bar{K}p$ is the 0.4-day mean of the 3-hourly planetary index Kp ; or that given recently by Jacchia, Slowey and von Zahn[22]

$$\Delta T = A \sin^4 \phi \qquad (11)$$

where $A = 57.5Kp\left[1 + 0.027 \exp 0.4Kp\right]$ kelvins, and ϕ is the latitude. Equation (10) gives a larger correction than equation (8) for latitudes greater than 30^o, and would therefore be more satisfactory for some of the values, for example at MJD 41953 and 41985. Equation (11) is unacceptable, however, because it gives zero effect at the equator, whereas Fig 6 shows that the storms between 41760 and 41780 are accompanied by density increases of about 20% and 30% respectively, although perigee is very near the equator.

The conclusion drawn is that the Ap index does not always adequately register the effects of magnetic storms on the upper atmosphere. However, the formula used here, equation (8), has compensated for the effects reasonably well, especially so in the major storms of August 1972 and July 1974.

6.2.3 Further recognizable recurrent variations

Comparing the density index curves for the years 1972-74, after allowance is made for the semi-annual variation and any residual variations at times of geomagnetic disturbances, other features which recur in each of the three years become apparent.

Between the March-April maximum and the July-August minimum Figs 5 to 7 reveal a subsidiary minimum and maximum, with the minima at about June 2, May 25 and May 25 for the years 1972, 1973 and 1974 respectively, and the maxima about July 2, June 15 and June 10. This 'June revival' in density also seems to occur in 1968-71: from analysis of 1967-31A, there is[23] a minimum near May 25 and a maximum near June 15 in 1968 and[4] a minimum near May 18 and maximum near June 15 in 1969; analysis of 1969-108A[5] indicates a minimum around May 25 and a maximum about June 25 in 1970; and the analysis of 1970-65D, indicates a minimum near May 29 and maximum near June 28 in 1971. So the 'June revival' shows itself in seven successive years, with minimum and maximum around May 26 and June 20 respectively. There is also some evidence of this 'June revival' in earlier years from the data in 1966-69 presented by Wulf-Mathies[24] and in the average values for the 1960s of Jacchia and Slowey[19].

Two more similarities are worth a mention: first, there is a group of values below the semi-annual band from 14-23 November; second, another group lies above the semi-annual band from 19-27 December. This feature is apparent in all three years and also in the results from 1969-20B[6] for 1969. Results for the years 1971 and 1972 are not available in sufficient detail to determine if the same trend is present.

6.3 Variation of density with height

The variation of density, ρ_A, with height is given in Fig 12. For dates before 13 March 1975 (when $y > 208$ km) the values of ρ_A plotted are those near the averages of both the semi-annual variation and the day-to-night variation, defined as the values of ρ_A when $0.95 < D < 1.05$ and $1.12 < T_\ell/T_c < 1.18$, and also when geomagnetic disturbances are small, $Ap < 30$. After 13 March 1975 all the points are plotted except those with $Ap > 30$; the points plotted are values of ρ_λ, because $e < 3H^*/a$ (see section 4.1).

The values of density are plotted with different symbols to indicate into which bands of exospheric temperature they fall. The three curves drawn represent the *CIRA 1972* values of density for exospheric temperatures of 800, 900 and 1000 kelvins.

Fig 12 shows there is good agreement between the observational points and the curves of *CIRA 1972*. Agreement at heights near 245 km is to be expected, because the value of δ was chosen to give densities consistent with *CIRA* at that height. Fig 12 therefore shows that *CIRA 1972* gives the correct variation of density with height between 250 km and 175 km.

7 DISCUSSION

7.1 Solar activity and diurnal variations

Inspection of Figs 5 to 8 reveals that the variations due to solar activity and diurnal variations have been successfully removed.

The values of $F_{10.7}$ have been used (section 5.2.1) to remove the variations due to solar activity from the ρ_B values, and the graph of density index shows no correlation with $F_{10.7}$. For example in Fig 5 at MJD 41360 there is a steep rise in ρ_{245} to a peak at MJD 41370, corresponding to a similar rise in $F_{10.7}$; a look at the values of D shows that this increase has been successfully removed.

078 The diurnal variations give a maximum in density around 14 h local time and a minimum at 03 h local time. This variation is visible in ρ_B but no

trace of it (or over-correction of it) is discernible in the values of D , so it can be assumed that this variation is correctly modelled in *CIRA 1972*. The amplitude of the exospheric temperature day-to-night variation is taken as 0.3 in *CIRA 1972*, but Broglio *et al*[25] have suggested that this value should vary with altitude and give a value of 0.19 at 240 km height decreasing to 0.14 at 210 km height; however, there is no indication that this change is needed in the present study.

7.2 Effects of geomagnetic disturbance

The increases in density at times of geomagnetic disturbance have been allowed for by using equation (8) (see section 5.2.3). The increases in density have not always been completely removed and various reasons are possible. Nisbet *et al*[26] suggest that the effects of geomagnetic activity are stronger in the morning than the afternoon. At the times of six geomagnetic storms, MJD 41438, 41865, 41985, 42280, 42335 and 42360, the effects of geomagnetic activity have not been completely removed from the density index values, but as three of these storms occurred in the morning and three in the afternoon the suggestion of Nisbet *et al* does not seem to apply here. A second possibility is that equation (8) should include some effect of latitude, but, as already explained in section 6.2.2, the use of latitude-dependent equations is unhelpful. Trinks *et al*[27] conclude that the global geomagnetic index is inappropriate for correlation with locally confined data. This confirms the conclusion of section 6.2.2 as the most likely reason for the incomplete removal of the storm effects, as all the values of density calculated here are for a localized section of the orbit - an arc of 40^{o} centred on perigee.

7.3 Year-to-year variations in semi-annual effect

From the analysis of satellite orbits during the 1960s a three-year oscillation in the strength of the semi-annual variation was detected. King-Hele and Walker[28] first suggested that the amplitude of the semi-annual variation oscillated with a period of about 33 months, with maxima in early 1959, late 1961, and 1964; and Cook[3,29] showed that a three-year periodicity existed from 1958 to 1967. Voiskovskii *et al*[30] give semi-annual variations at 240 km height derived from analysis of the orbits of Cosmos satellites, and their amplitudes have clear maxima in 1964 and 1967; but for the years 1968-70 the picture is less clear. Marov and Alpherov[31] give results from Cosmos satellites from 1961 to 1969, which again show maxima in 1964 and 1967. Wulf-Mathies *et al* [32] give the results from analysis of Explorers 19, 24 and 39, which also show a large semi-annual effect in 1967. 078

In Fig 13 the results given in Table 3 are combined with others from 1966 to 1972 [4-8,33-35]. Mean values have been taken of the ratio of the October maximum to the following January minimum and April maximum to the same January minimum each year, and the values are plotted as triangles joined by a dashed line. Similarly mean values of April maximum to July minimum and October maximum to July minimum each year are obtained and plotted as circles joined by a dash-dot line. The full line in Fig 13 is the mean of the two curves already mentioned and should represent the year-to-year changes in the amplitude of the semi-annual variation. The 1967 maximum is clearly visible but there is no maximum in 1970 as would be expected, and after 1971 the value remains almost constant with average value 1.48 ±0.04.

So the three-year oscillation apparent in the 1960s disappeared during the first half of the 1970s.

7.4 Standardized semi-annual variation for 1972-4

The results show a semi-annual variation which differs considerably from that of *CIRA 1972* and also agrees with the results in 1970-71 [7] that the April maximum was stronger than October maximum. So it is worth trying to construct a standardized semi-annual variation in density for 1972-74 at heights of 200-250 km.

Fig 14a shows the variation of $\bar{D}$, the value of the density index D given by curves midway between the dashed curves in Figs 5 to 8. The choice of a standard curve for $\bar{D}$ is difficult, but as the individual values at each particular maximum and minimum are within 5% of the mean values, the standard curve has been constructed by adopting the mean maximum and minimum values given in Table 2 and choosing dates which are acceptable for the majority of the years. Fig 14b shows this standard curve: the dates above the curve are the mean dates of the maximum and minimum given in Table 2. The actual dates from the standard curve for the January minimum, April maximum, July minimum and October-November maximum, given below the curve in Fig 14b, are January 24, April 5, July 21 and November 5. As it happens the only major departure from the mean dates given in Table 2 is that for the January minimum; this is ten days earlier than the mean date of Table 2, and gives more weight to the results for 1973 and 1974 obtained here, the date for 1971 [7] (January 5) and the date (January 16) for the 1960s given by *CIRA 1972* [1]. Although the recommended curve does not apply for any single calendar year, it is close to the variation during the twelve months starting on 1 September 1972.

078

Fig 14b is offered as a method of determining density in the early 1970s: first, density ρ_{CIRA} should be calculated from *CIRA 1972*, taking account of the appropriate local time, latitude, solar activity and geomagnetic disturbance but ignoring the *CIRA* semi-annual variation. Then ρ_{CIRA} should be multiplied by the standardized $\bar{D}$ of Fig 14b. The results apply for heights of 200-250 km, but the semi-annual effect is not strongly dependent on height and the results may be valid down to about 150 km and up to 300 km. As the actual semi-annual variation differs from that of *CIRA*, there is no reason why the mean value of the standardized $\bar{D}$ over a year should be 1.0: the actual mean value in Fig 14b is 1.030.

7.5 Possible explanations for the semi-annual variation

Many theories for the origin of the semi-annual variation have been propounded, but none of them offers a complete explanation. In 1969 Cook[3] discussed in detail numerous explanations proposed in the 1960s, and emphasized the continuation of the effect down to about 90 km; but he concluded that the semi-annual effect should be regarded as "one of the least understood phenomena of the atmosphere".

The name 'semi-annual variation' describes an effect that really comprises two variations - one annual and the other (and larger) semi-annual. An annual variation arises because of the variation in the Earth's distance from the Sun; the solar radiation received in January is 7% greater than in July, so the density in January at heights near 240 km is expected to be about 8% greater than in July. This accounts for much of the difference between the January and July values, but the semi-annual variation remains to be explained.

Of the various explanations of the semi-annual effect that have been proposed, the most promising seem to be those which attribute the effect to seasonal-latitudinal variations in the mesosphere extending into the thermosphere. Volland[36] compared the effects produced by heating at various heights in the thermosphere and concluded that the variation of the semi-annual effect with height was best modelled by heat input at the base of the thermosphere. He suggested that a leakage of wave energy flux of a tidal wave into the thermosphere from the lower atmosphere, due to changes in mesospheric wind systems which are often semi-annual in character, produces the observed density variations. Marov and Alpherov[31] conclude that the semi-annual density variations in the thermosphere are linked with seasonal circulation of the lower atmosphere. Ching and Chiu[37] point out that the total solar radiation impinging on the Earth, in both the lower and upper atmosphere, has a semi-annual variability. Fukuyama[38]

finds a semi-annual variation in night airglow intensity, which supports the view of linkage between lower and upper atmosphere. Groves[39] has described semi-annual variations in density in the 100-km region which link with the thermospheric semi-annual variation. Groves[40] has also investigated the absorption of solar radiation by water vapour and ozone, and concluded that the observed variations, particularly the low value in July, agree with the thermospheric semi-annual variation.

7.6 Comparison with Jacchia's new models (1977)

After the completion of this work, Jacchia's latest atmospheric models[41] were issued. He states that, in selecting the form and amplitude of the semi-annual variation, "we still prefer to use the model of J71", which is the same as the *CIRA 1972* model. However, the tables he gives show a slightly increased amplitude: the values at the January minimum, April maximum, July minimum and October maximum for comparison with those of Table 2 are 0.94, 1.14, 0.83 and 1.18 respectively. Jacchia's new values are therefore generally nearer than those of *CIRA 1972* to the variations found here for 1972-5, but the amplitude is still too small: in particular his ratio of the April maximum to the July minimum is 1.37, as opposed to 1.68 found here.

8 CONCLUSIONS

Analysis of the orbit of 1971-106A during its 40-month lifetime has yielded 604 values of air density at heights near 200 km.

Variations in the density values due to solar activity and diurnal variations have been successfully removed using *CIRA 1972*. Allowance was also made for the increases in density at times of geomagnetic disturbances using *CIRA 1972* (see section 5.2.3), but this was not always so successful and various possible reasons have been given (section 7.2). After removal of these effects and conversion of density to a standard height, a record of the residual variations in density between January 1972 and April 1975 emerges.

The main residual variation has a semi-annual pattern and the maximum and minimum values of the variation are given in Table 2. The results show that:

(1) There is only a small variation from year to year in the value of the density index at a particular maximum or minimum of the semi-annual variation; but three of the mean values are significantly different from those of *CIRA 1972*, always giving a stronger variation than *CIRA*.

(2) The October maxima are all lower than the April maxima, the mean value being 5% lower. This does not conform with *CIRA 1972* where the October maximum is 4% higher than the April value.

(3) As in *CIRA 1972*, the July minima are stronger than the January minima, but 18% stronger where *CIRA* gives 10%.

(4) The shape of the variation is not sinusoidal and the maxima and minima are not at regular intervals.

(5) When the ratio of the April maximum to January and July minima and the ratio of the October maximum to the July and following January minima are compared (see Table 3), the values for each individual ratio for each of the three years are surprisingly constant, in contrast to the 1960s, when there were wide variations from year to year. The ratios of maximum/minimum density in 1972-5 are greater than those of *CIRA 1972*, and close to the average of the maximum values of the ratios in the 1960s (see Fig 13).

The variation of density with height between 176 and 252 km obtained from analysis of 1971-106A is in close agreement with the *CIRA 1972* model (see Fig 12).

In addition to the main semi-annual variation, the air density shows three other recurrent features. The most important is a minimum in late May and a maximum in mid June. There is also a mid-November minimum and a late-December maximum (see section 6.2.3).

Since the amplitude of the semi-annual variation in 1972-5 is so consistent, a standardized curve for the semi-annual variation in the early 1970s is presented (Fig 14), applying for heights of 200-250 km.

REFERENCES

No.	Author	Title, etc
1	-	*CIRA 1972* (Cospar International Reference Atmosphere 1972). (Akademie-Verlag, Berlin (1972)
2	H.K. Paetzold H. Zschörner	The structure of the upper atmosphere and its variations after satellite observations. *Space Research II*, pp 958-973 North-Holland Publ. Co, Amsterdam (1961)
3	G.E. Cook	The semi-annual variation in the upper atmosphere: a review. *Annales de Géophysique*, 25, 451-469 (1969) RAE Technical Report 69074 (1969)
4	D.G. King-Hele D.M.C. Walker	Air density at heights near 180 km in 1968 and 1969, from the orbit of 1967-31A. *Planet. Space Sci.*, 19, 297-311 (1971) RAE Technical Report 70084 (1970)
5	D.G. King-Hele D.M.C. Walker	Air density at heights near 150 km in 1970, from the orbit of Cosmos 316 (1969-108A). *Planet. Space Sci.*, 19, 1637-1651 (1971) RAE Technical Report 71129 (1971)
6	D.M.C. Walker	Air density at heights near 200 km from analysis of the orbit of 1969-20B. *Planet. Space Sci.*, 20, 2165-2173 (1972) RAE Technical Report 72071 (1972)
7	D.M.C. Walker	Air density at heights near 200 km from the orbit of 1970-65D. *Planet. Space Sci.*, 22, 403-411 (1974) RAE Technical Report 73098 (1973)
8	C.J. Brookes F.C.E. Ryland	Air density at heights near 300 km, from analysis of the orbit of China 2 rocket (1971-18B). *Planet. Space Sci.*, in press
9	L. Freedman	The Soviet Union and anti-space defence. *Survival*, XIX, No.1, 16-23 (1977)

REFERENCES (continued)

No.	Author	Title, etc
10	C.S. Sheldon II	*Soviet Space Programs, 1971-75* Volume 1, pp 424-429 US Govt. Printing Office, Washington (1976)
11	J.A. Pilkington D.G. King-Hele H. Hiller	Table of Earth satellites, Vol 2: 1969-1973. RAE Technical Report 74105 (1974)
12	D.M.C. Walker	Cosmos 462 (1971-106A): orbit determination and analysis. (to be published)
13	D.G. King-Hele G.E. Cook	Analysis of 27 satellite orbits to determine odd zonal harmonics in the geopotential. *Planet. Space Sci.*, 22, 645-672 (1974) RAE Technical Report 73153 (1973)
14	G.E. Cook	PROD, a computer program for predicting the development of drag-free satellite orbits. Part 1: theory. RAE Technical Report 71007 (1971) (*Celestial Mechanics*, 7, 301-314 (1973))
15	Y. Kozai	The motion of a close Earth satellite. *Astronom. Journ.*, 64, 367-377 (1959)
16	D.G. King-Hele	*Theory of satellite orbits in an atmosphere.* Butterworths, London (1964)
17	D.G. King-Hele	Improved formulae for determining upper-atmosphere density from the change in a satellite's orbital period. *Planet. Space Sci.*, 11, 261-268 (1963) RAE Technical Note No. Space 21 (1962)
18	J. Bartels	*IGY Annals*, Vol 4, pp 227-236 Pergamon Press, London (1957)
19	L.G. Jacchia J.W. Slowey I.G. Campbell	A study of the semi-annual density variation in the upper atmosphere from 1958 to 1966, based on satellite drag analysis. *Planet. Space Sci.*, 17, 49-60 (1969)
20	G. Rostoker	Geomagnetic indices. *Reviews of Geophysics and Space Physics*, 10, No.4, 935-950 (1972)

078

REFERENCES (continued)

No.	Author	Title, etc
21	M. Roemer	Geomagnetic activity effect on atmospheric density in the 250 to 800 km altitude region. *Space Research XI*, pp 965-974 Akademie-Verlag, Berlin (1971)
22	L.G. Jacchia J.W. Slowey U. von Zahn	Temperature, density, and composition in the disturbed thermosphere from Esro 4 gas analyzer measurements: a global model. *Journ. Geophys. Res.*, 82, 684-688 (1977)
23	B.R. Bowman	Variations in air density at heights near 200 km during 1967-1969, from the orbit of 1967-31A. *Planet. Space Sci.*, 23, 1659-1667 (1975)
24	C. Wulf-Mathies	Semi-annual variation of atmospheric densities near solar activity maximum. *Space Research XI*, pp 981-986 Akademie-Verlag, Berlin (1971)
25	L. Broglio C. Arduini C. Buongiorno U. Ponzi G. Ravelli	Diurnal density variations measured by the San Marco 3 satellite in the equatorial atmosphere. *Journ. Geophys. Res.*, 81, 1335-1349 (1976)
26	J.S. Nisbet B.J. Wydra C.A. Reber J.M. Luton	Global exospheric temperatures and densities under active solar conditions. *Planet. Space Sci.*, 25, 59-69 (1977)
27	H. Trinks S. Chandra N.W. Spencer U.von Zahn	A two-satellite study of the neutral atmosphere response to a major geomagnetic storm. *Journ. Geophys. Res.*, 81, 5013-5017 (1976)
28	D.G. King-Hele D.M.C. Walker	Air density at a height of 470 km between January 1967 and May 1968, from the orbit of the satellite 1966-118A. *Planet. Space Sci.*, 17, 197-215 (1969) RAE Technical Report 68184 (1968)
29	G.E. Cook	Density variations in the exosphere from June 1968 to December 1970. *Planet. Space Sci.*, 20, 473-482 (1972) RAE Technical Report 71150 (1971)

REFERENCES (continued)

No.	Author	Title, etc
30	M.I. Voiskovskii I.I. Volkov N.I. Gryazev B.V. Kugaenko V.M. Sinitsyn P.E. El'yasberg	An aspherical model for the upper-atmosphere density. *Cosmic Research*, 11, 62-70 (1973)
31	M.Ya. Marov A.M. Alpherov	Semi-annual density variations of the atmosphere at heights of 200-300 km. *Space Research XII*, pp 803-808 Akademie-Verlag, Berlin (1972)
32	C. Wulf-Mathies E.J. Prior G.M. Keating	Annual and semi-annual density variations in the Earth's exosphere. *Space Research XV*, pp 279-285 Akademie-Verlag, Berlin (1975)
33	G.E. Cook	The semi-annual variation in the upper atmosphere during 1967 and 1968. *Planet. Space Sci.*, 18, 1573-1584 (1970) RAE Technical Report 69254 (1969)
34	D.G. King-Hele D.M.C. Walker	Air density at heights of 140-180 km, from analysis of the orbit of 1968-59A. *Planet. Space Sci.*, 17, 1539-1556 (1969) RAE Technical Report 69030 (1969)
35	D.G. King-Hele J. Hingston	Air density at heights near 190 km in 1966-7, from the orbit of Secor 6. *Planet. Space Sci.*, 16, 675-691 (1968) RAE Technical Report 67285 (1967)
36	H. Volland	A theory of thermospheric dynamics - I and II. *Planet. Space Sci.*, 17, 1581-1597, 1709-1724 (1969)
37	B.K. Ching Y.T. Chiu	Annual and sub-annual effects of EUV heating Volumes I and II. Aerospace Corporation Report TR-0172(2260-10)-9 (1972)
38	K. Fukuyama	Airglow variations and dynamics in the lower thermosphere and upper mesosphere. II. Seasonal and long-term variations. *Journ. Atmos. Terr. Phys.*, 39, 1-14 (1977)

REFERENCES (concluded)

No.	Author	Title, etc
39	G.V. Groves	Annual and semi-annual zonal wind components and corresponding temperature and density variations, 60-130 km. *Planet. Space Sci.*, 20, 2099-2112 (1972)
40	G.V. Groves	Energy fluxes propagated by diurnal oscillations in the upper atmosphere. *Journ. Brit. Interplan. Soc.*, 30, 32-36 (1977)
41	L.G. Jacchia	Thermospheric temperature, density, and composition: new models. Smithsonian Astrophysical Observatory Special Report 375 (1977)

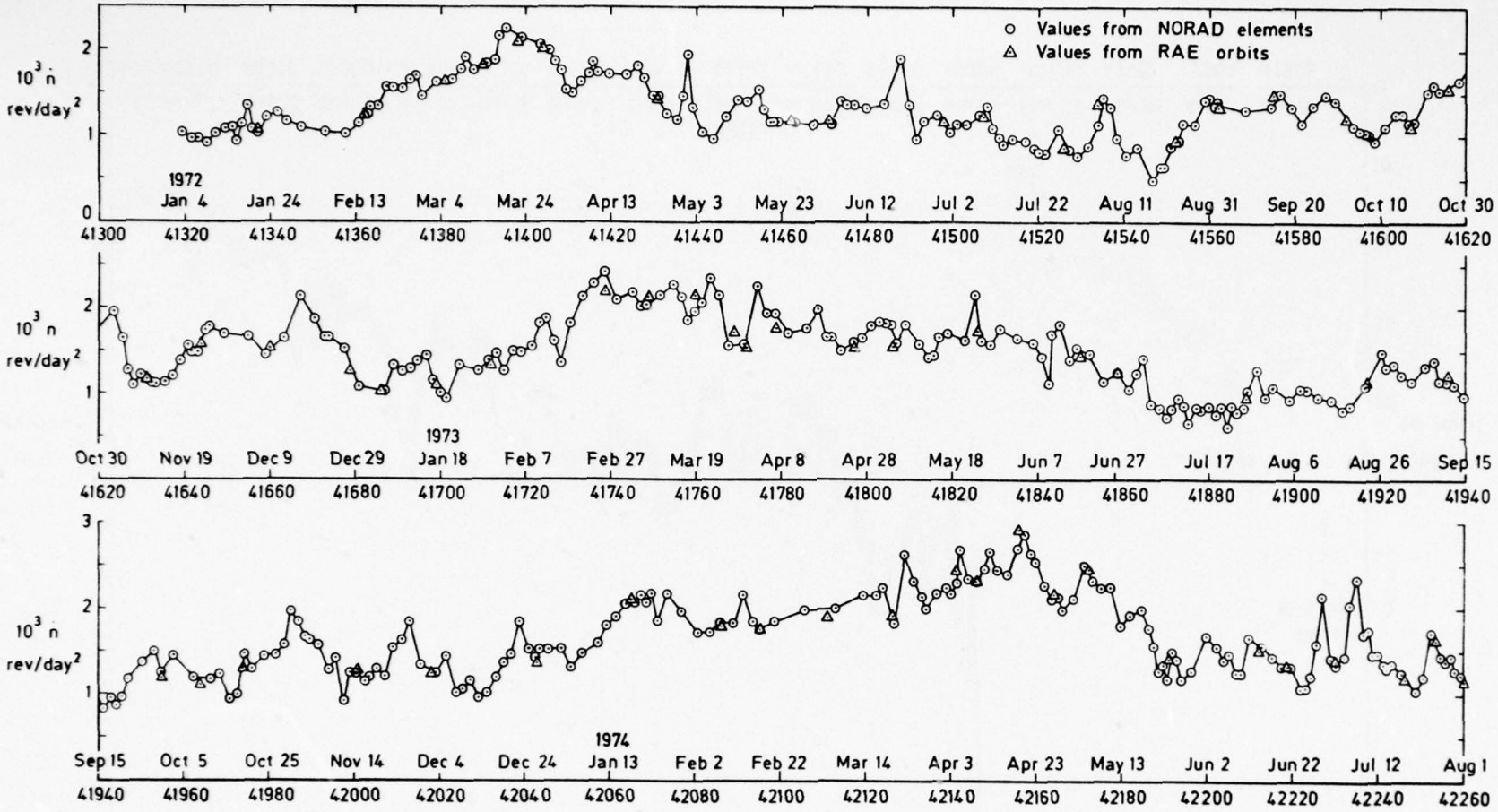

Fig 1 Orbital decay rate ṅ for Cosmos 462, from January 1972 to July 1974

Fig 1

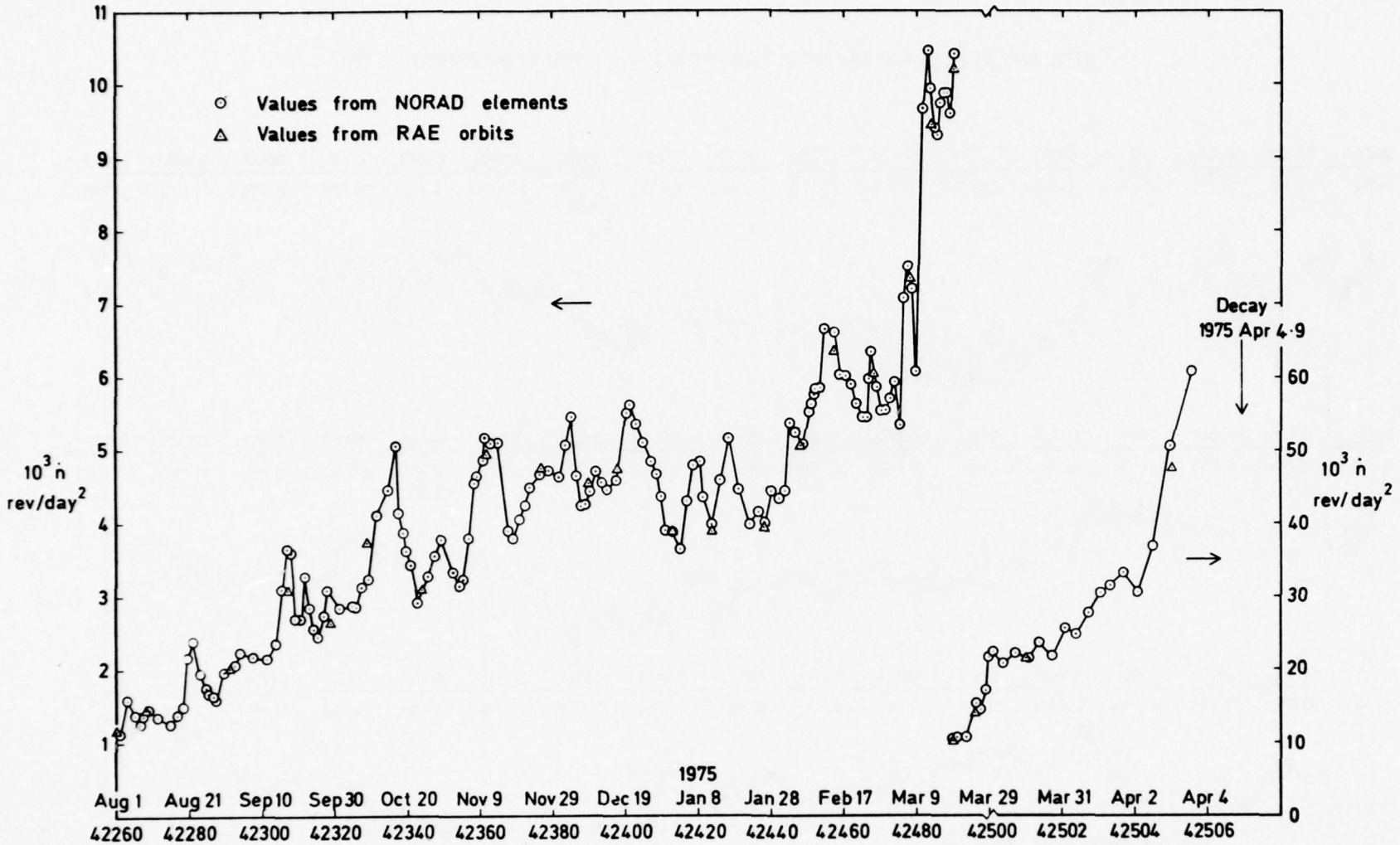

Fig 2 *Orbital decay rate $\dot{n}$ for Cosmos 462, from August 1974 to April 1975*

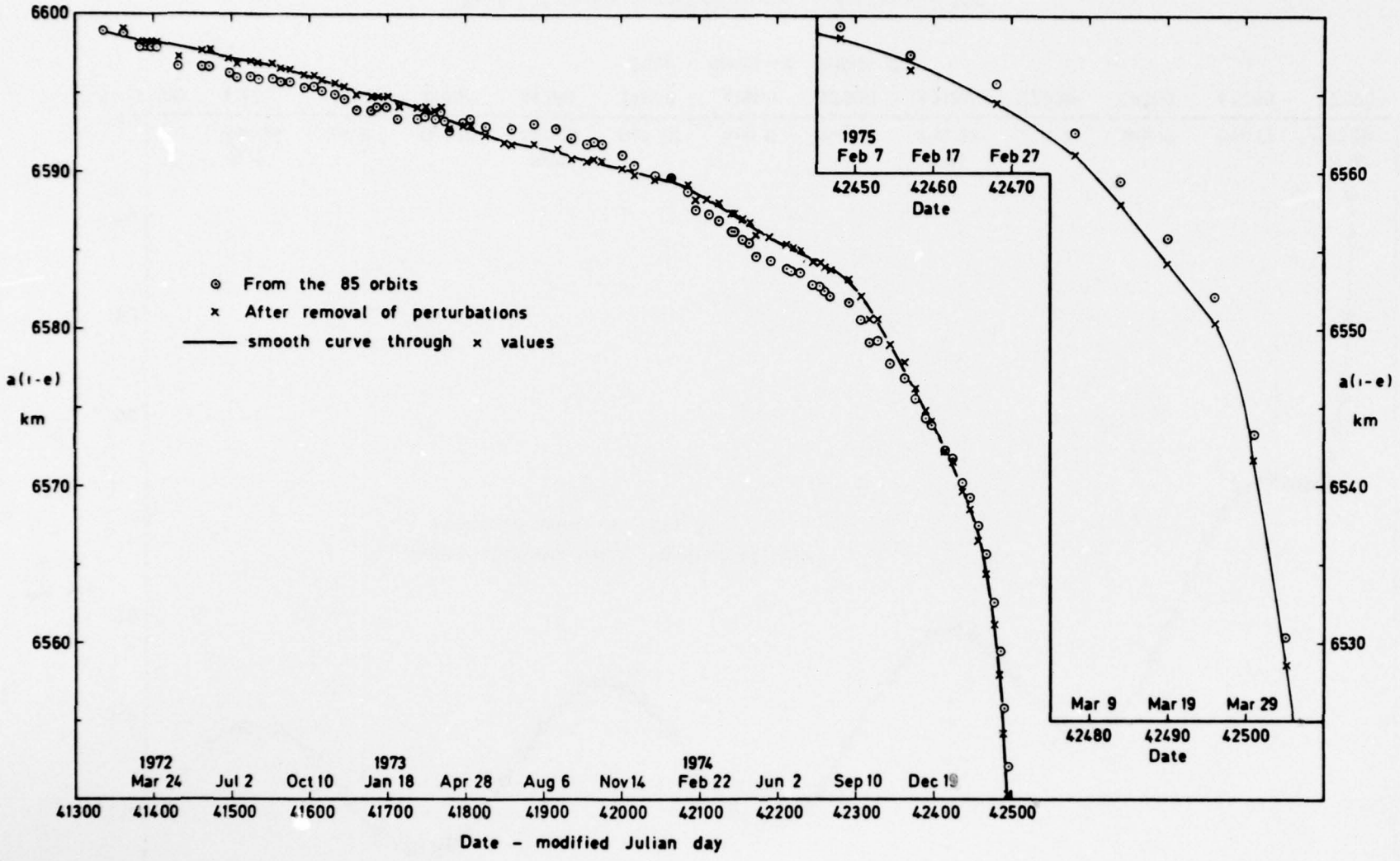

Fig 3 Values of $a(1-e)$ for Cosmos 462

Fig 3

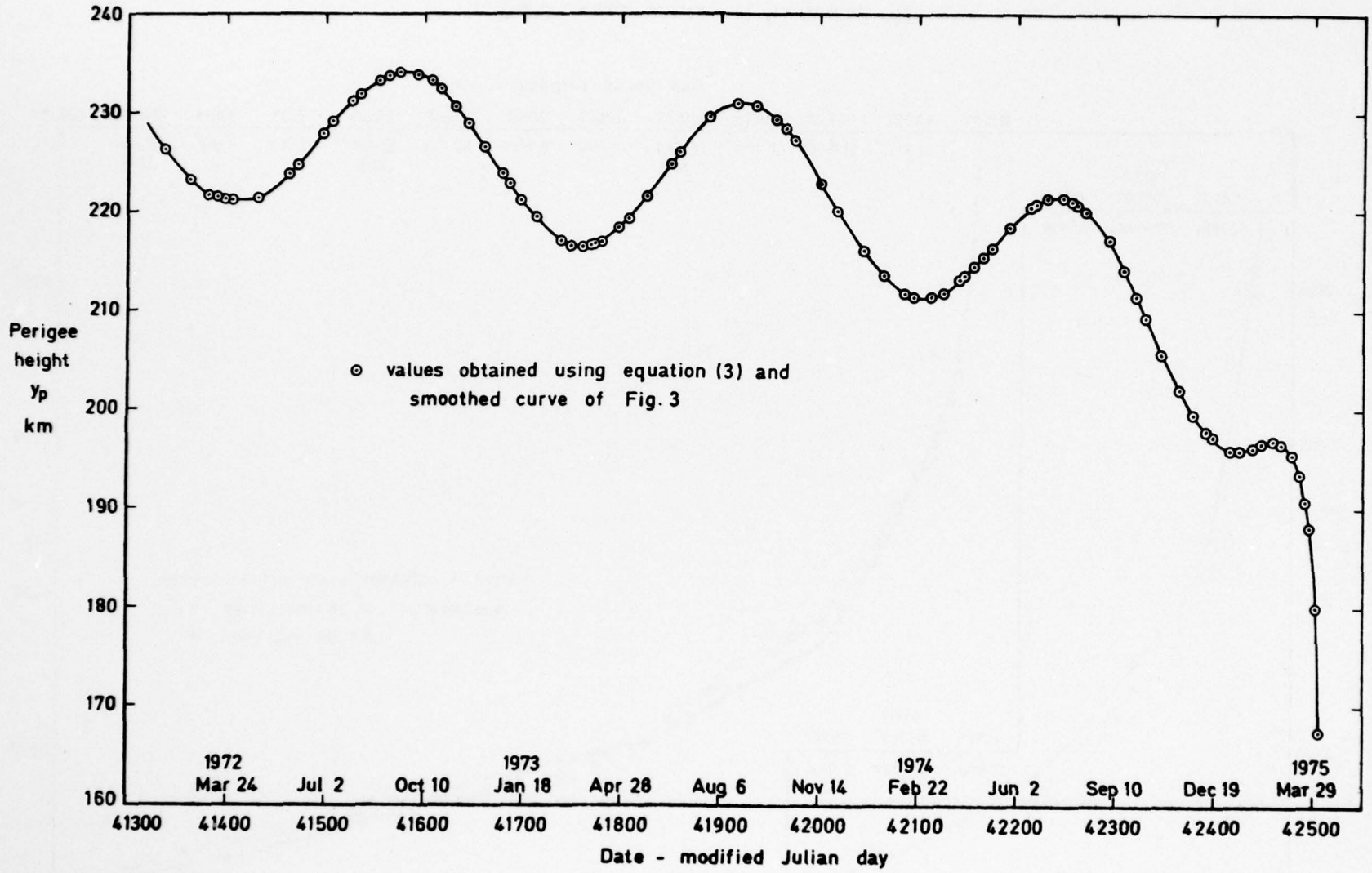

Fig 4 Variation of perigee height y_p for Cosmos 462

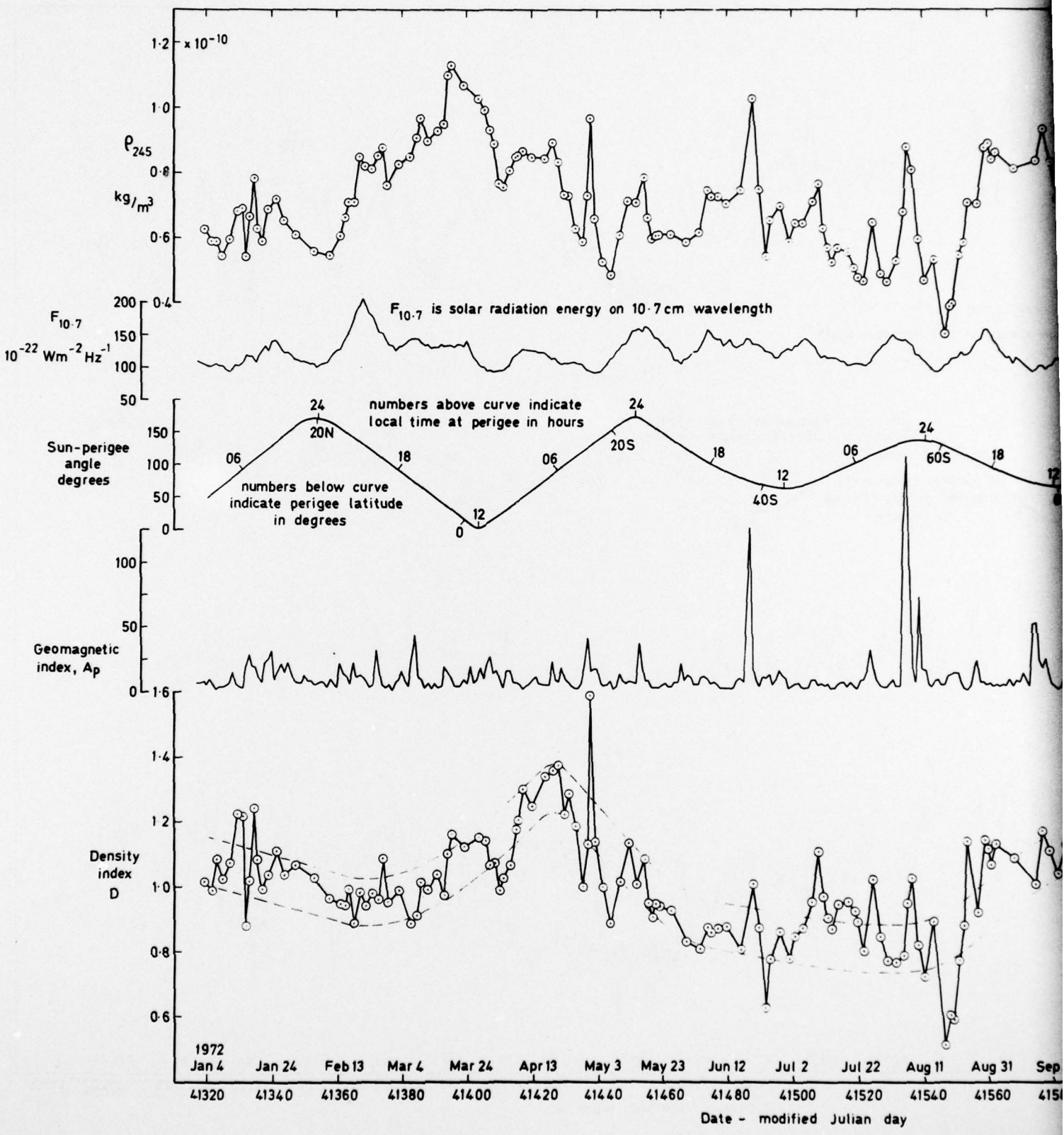

Fig 5 Values of density at a height of 245 km in 1972, ρ_{245}, and density index D, v radiation energy $F_{10.7}$, Sun-perigee angle and geomagnetic index Ap

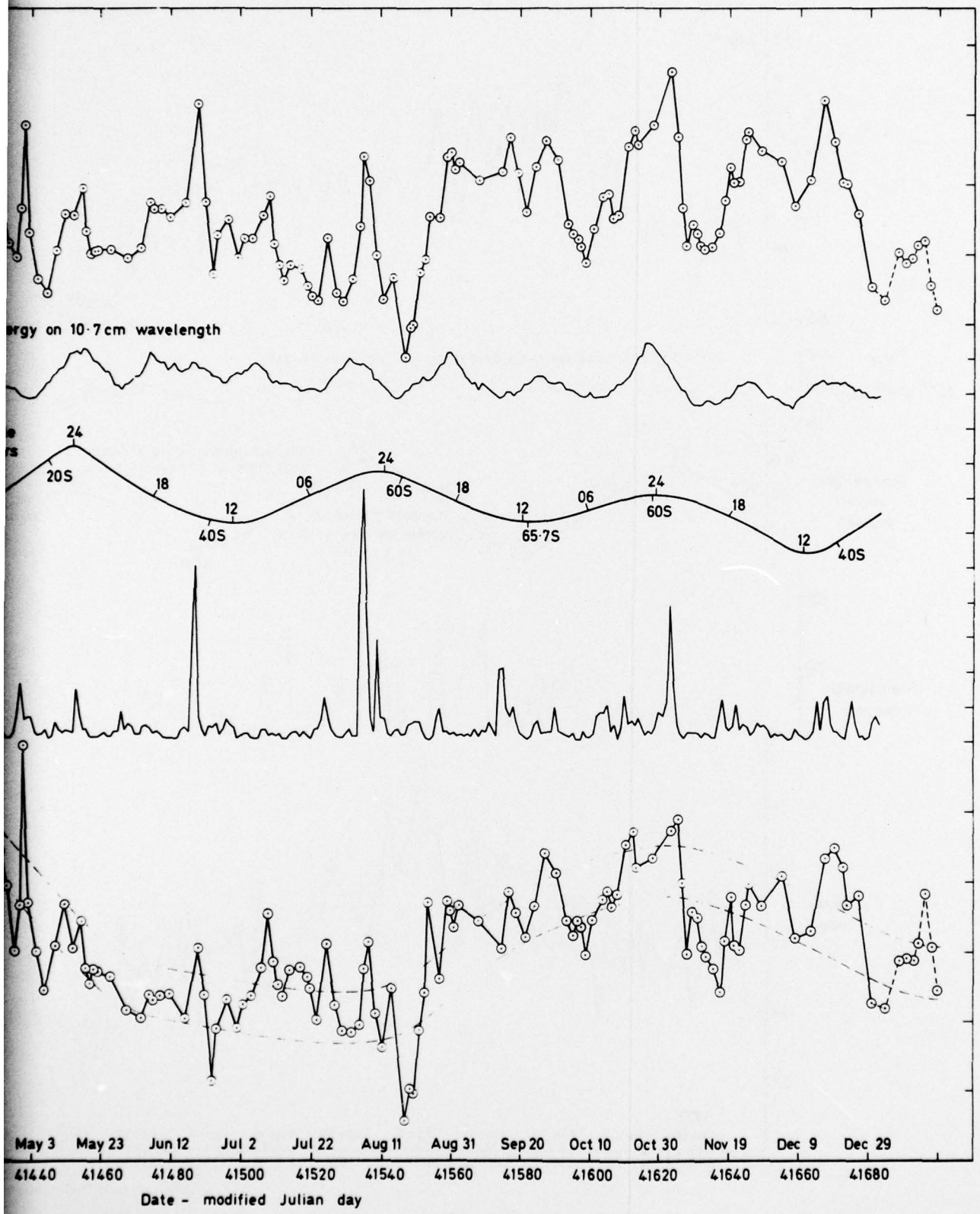

a height of 245 km in 1972, ρ_{245}, and density index D , with solar
0.7 , Sun-perigee angle and geomagnetic index Ap

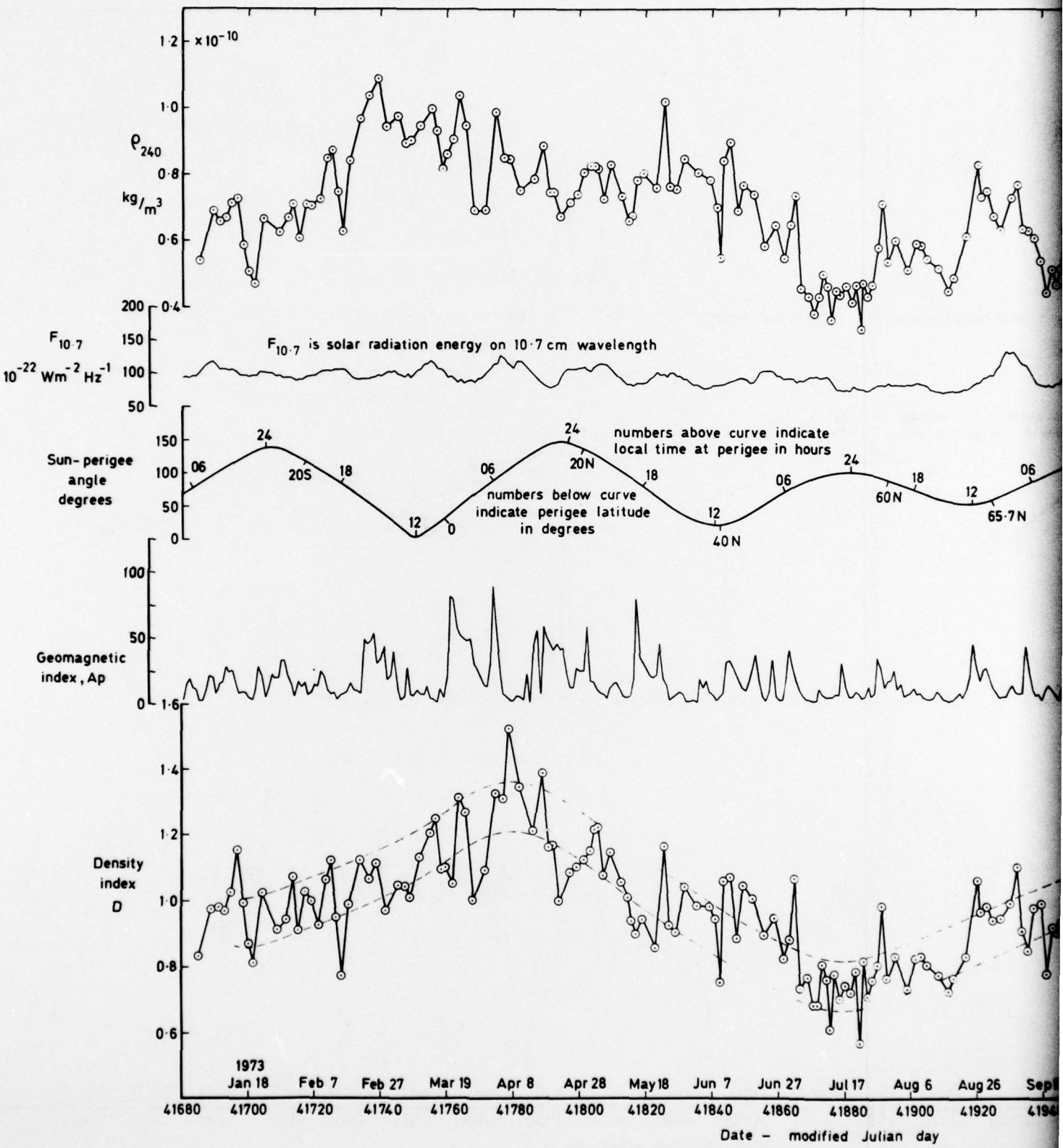

Fig 6 Values of density at a height of 240 km in 1973, ρ_{240}, and density index D, radiation energy $F_{10.7}$, Sun-perigee angle and geomagnetic index Ap

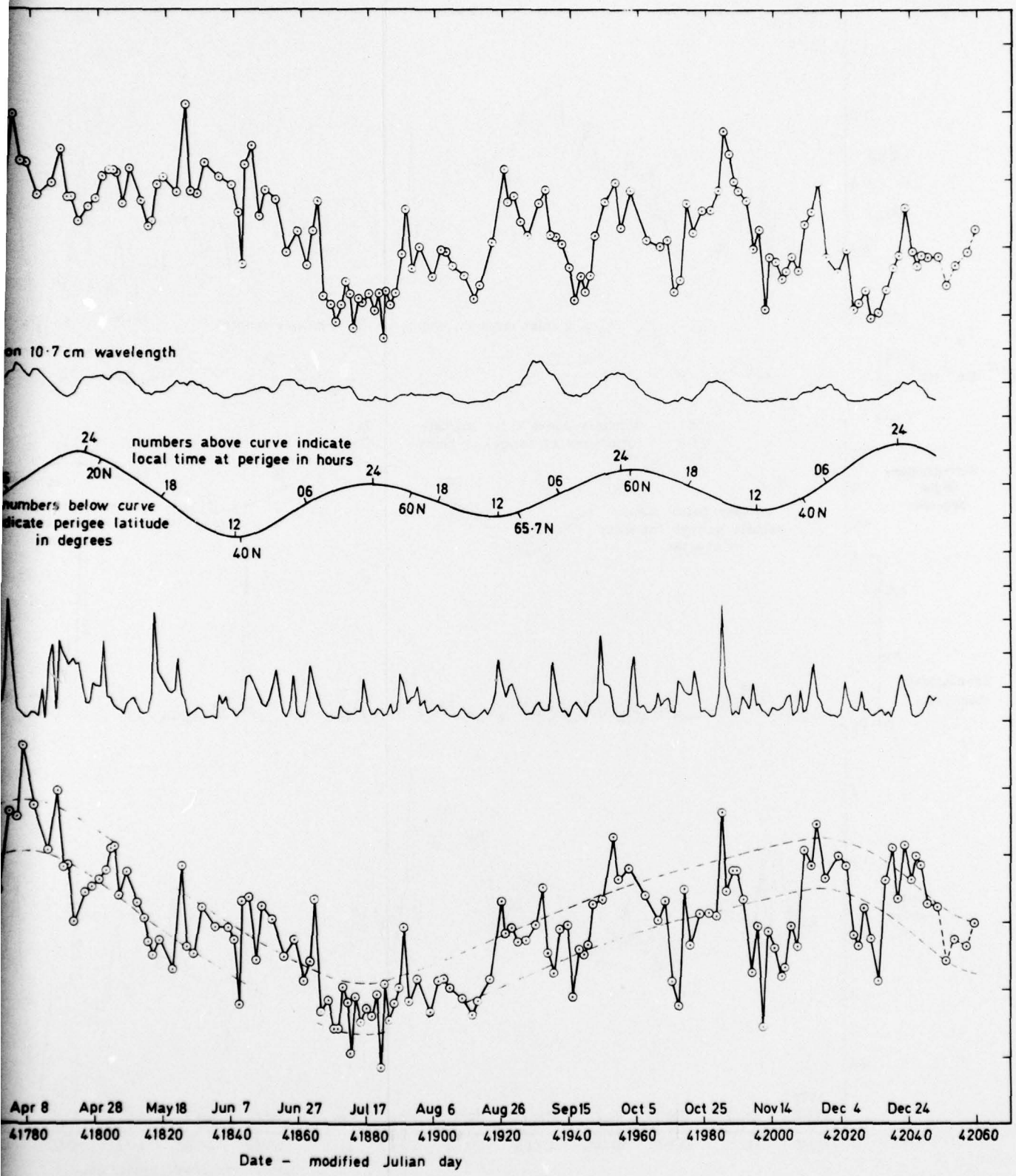

density at a height of 240 km in 1973, ρ_{240}, and density index D , with solar
nergy $F_{10.7}$, Sun-perigee angle and geomagnetic index Ap

2

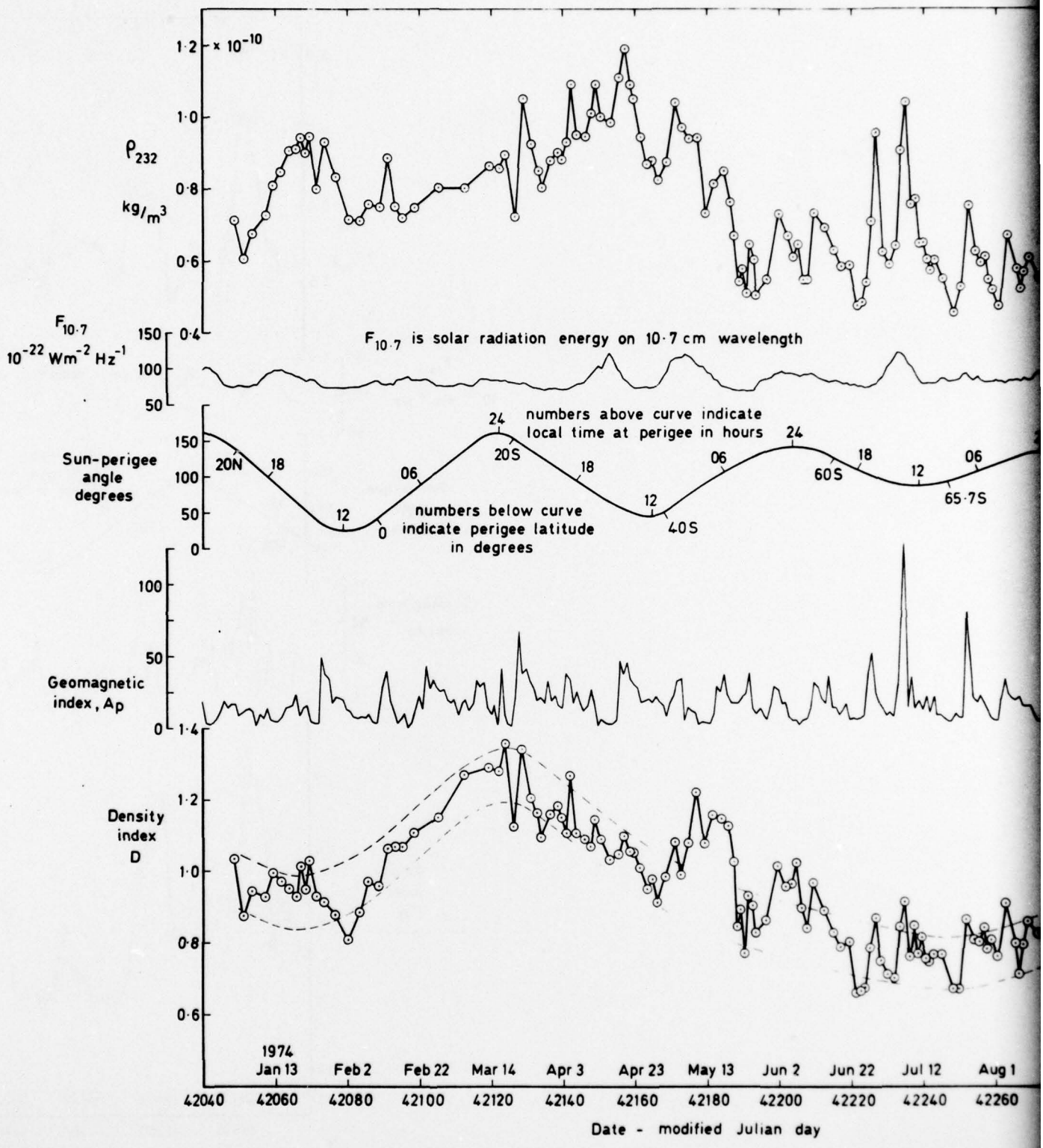

Fig 7 Values of density at a height 232 km, ρ_{232}, from 1 January to 30 September 1974, and density index D, with solar radiation energy $F_{10.7}$, Sun-perigee angle and geomagnetic index Ap

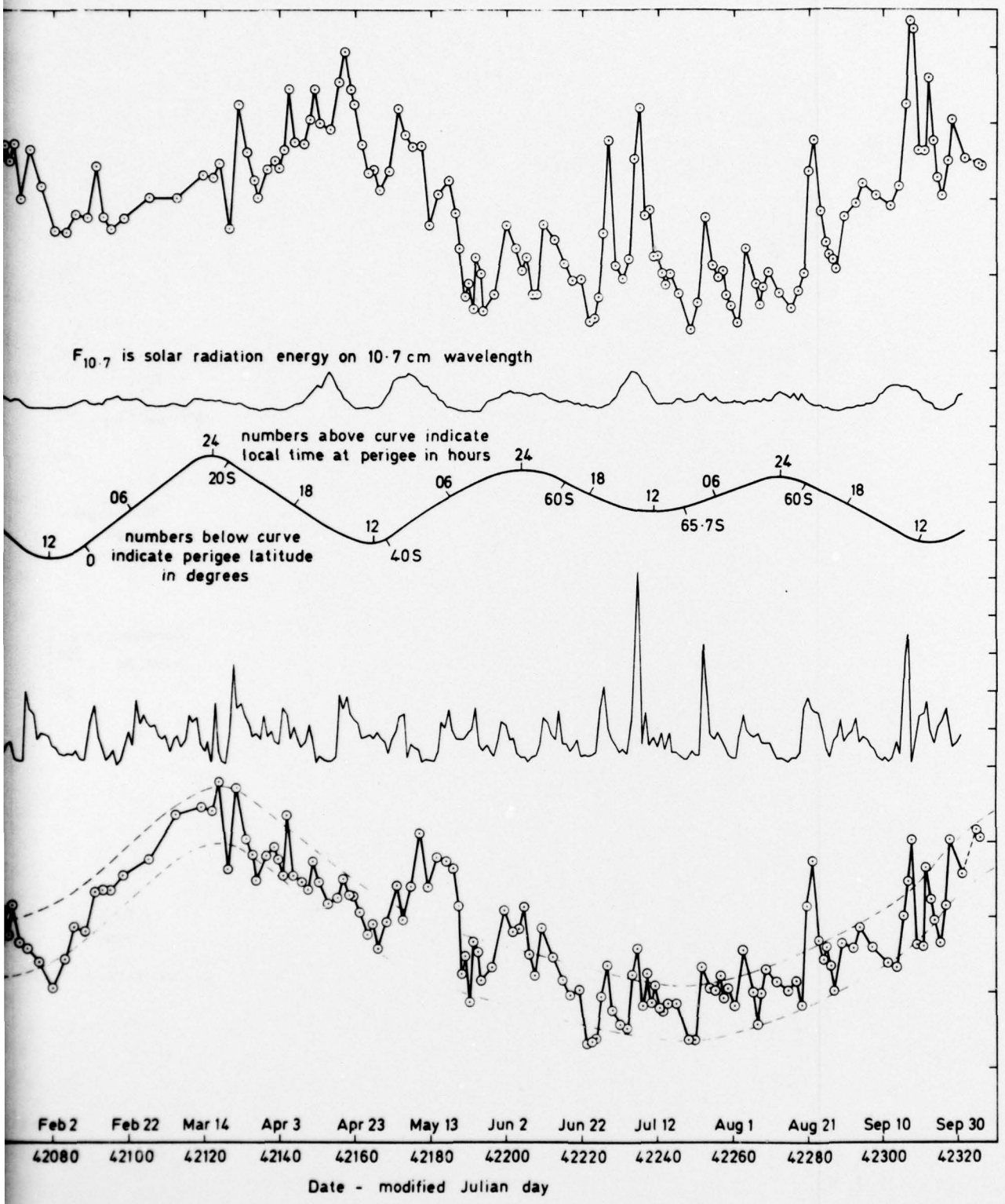

Values of density at a height 232 km, ρ_{232}, from 1 January to 30 September 1974, and density index D, with solar radiation energy $F_{10.7}$, Sun-perigee angle and geomagnetic index Ap

2

Fig 8

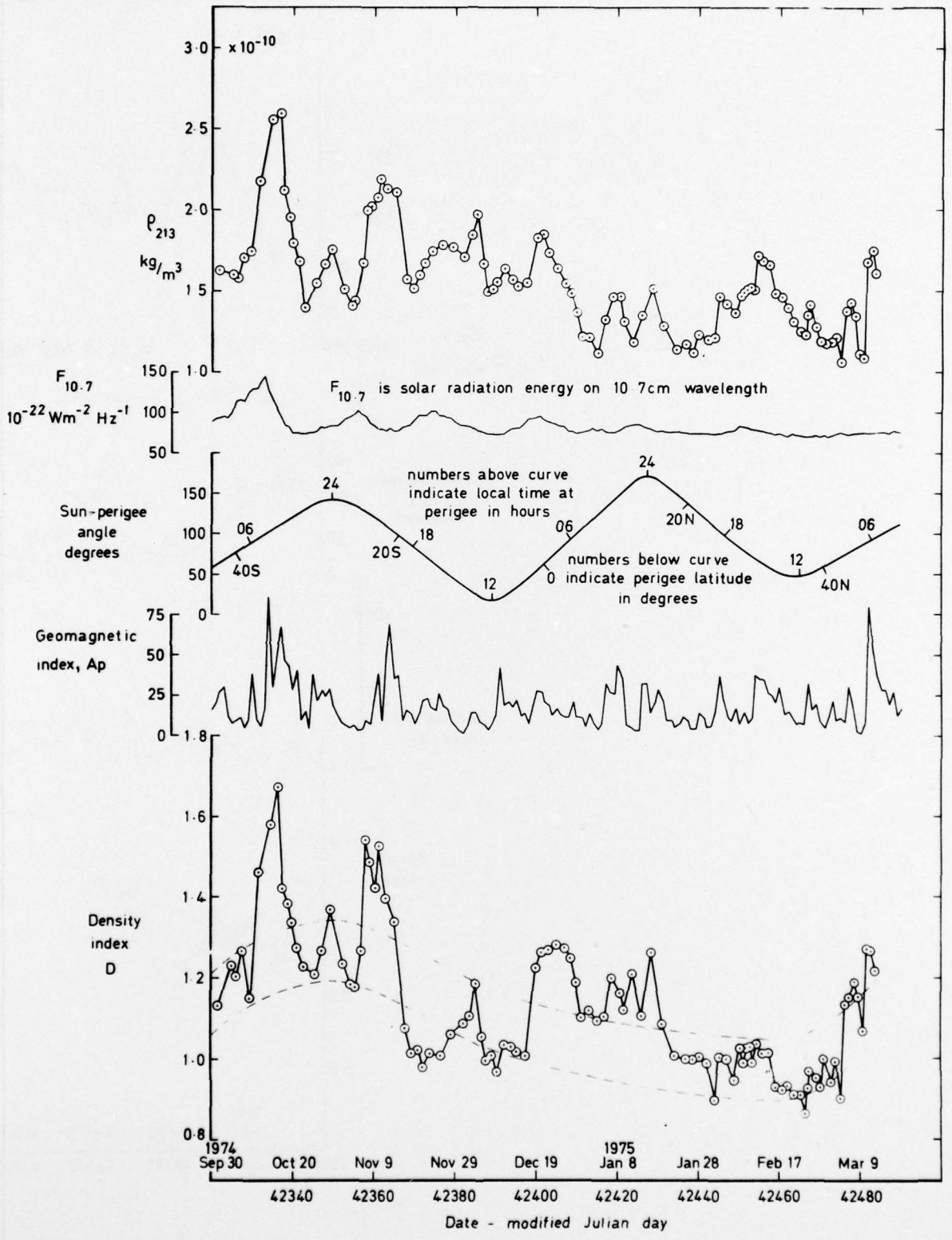

Fig 8 Values of density at a height of 213 km, ρ_{213}, from 1 October 1974 to 12 March 1975, and density index D, with solar radiation energy $F_{10.7}$, Sun-perigee angle and geomagnetic index Ap

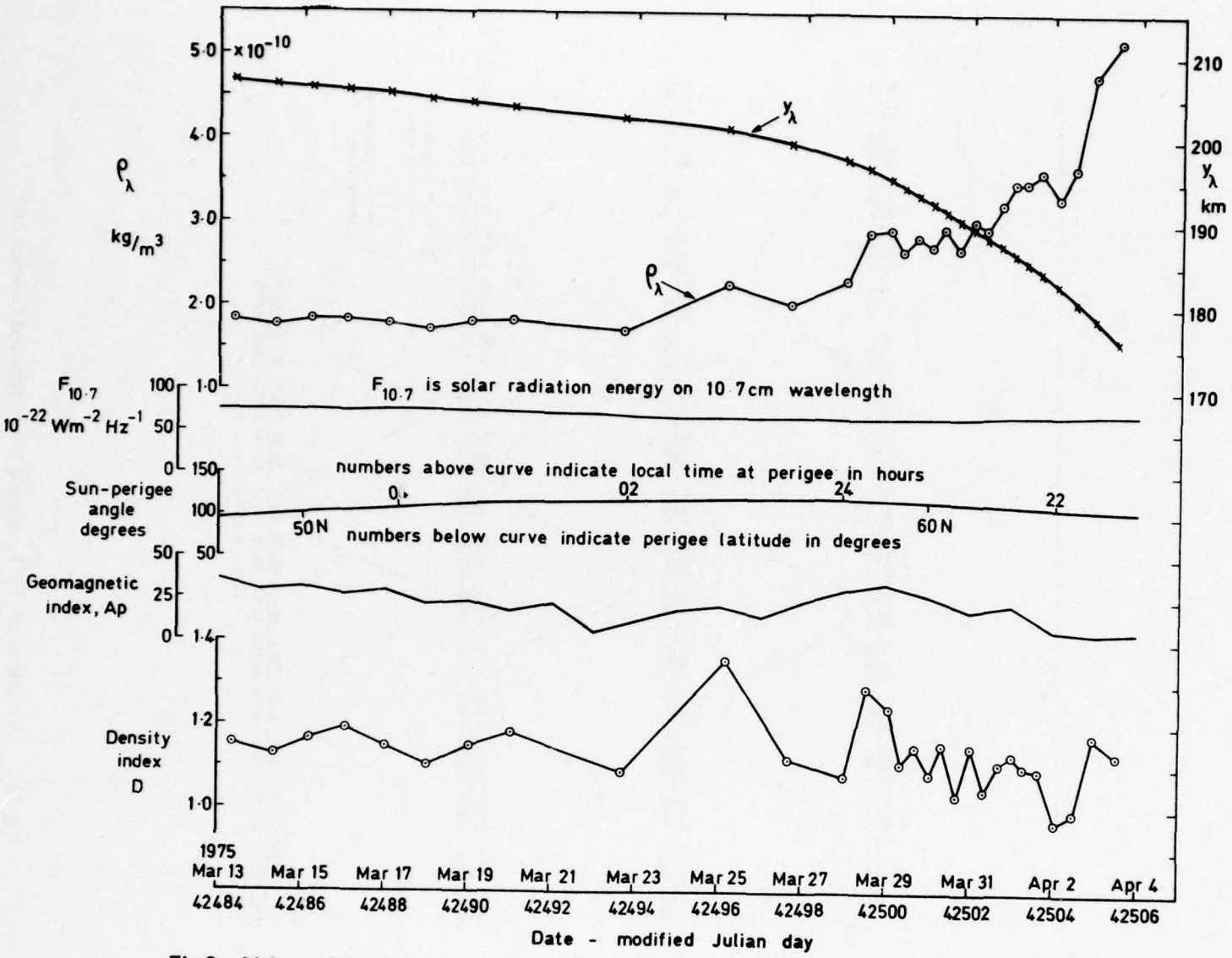

Fig 9 Values of density ρ_λ at height y_A, from 13 March to 4 April 1975, and density index D, with solar radiation energy $F_{10.7}$, Sun-perigee angle and geomagnetic index Ap

Fig 10

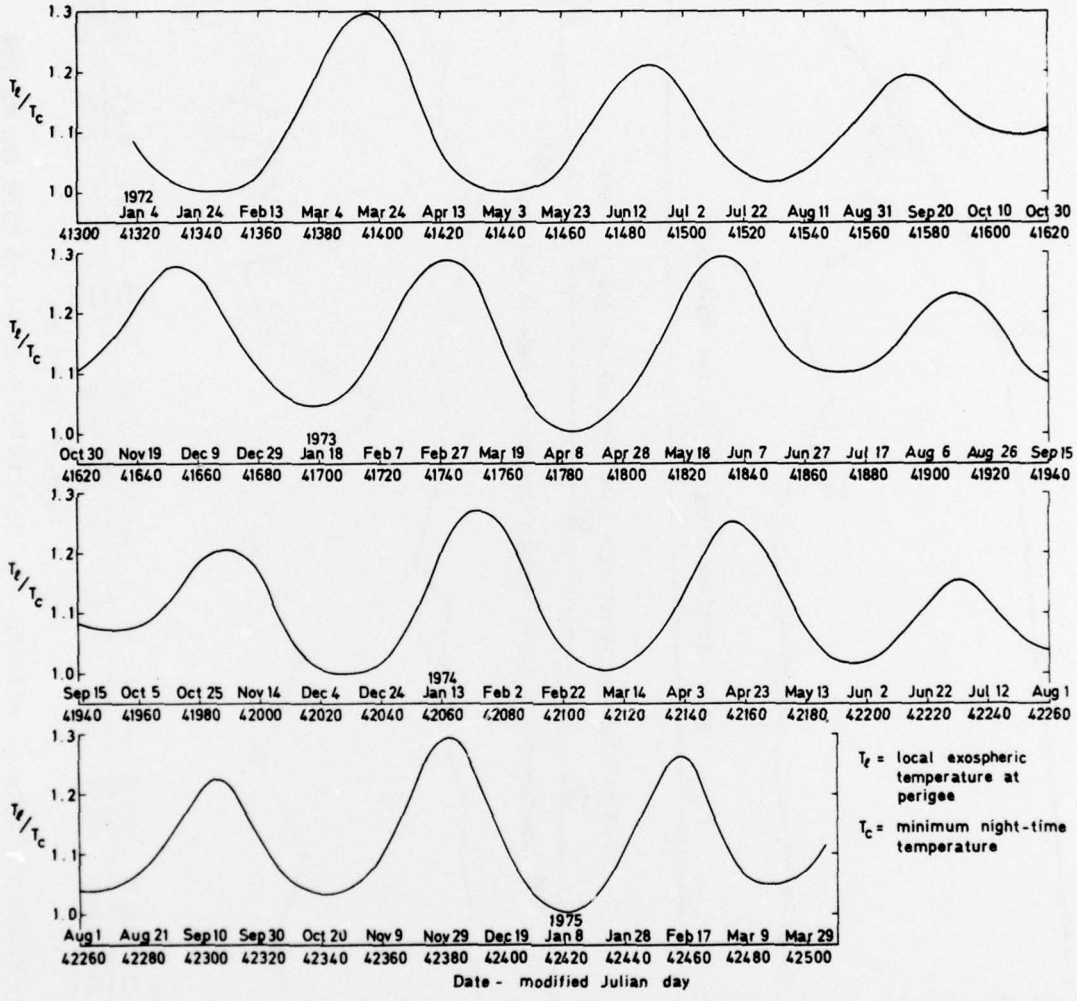

Fig 10 Variation of T_ℓ/T_c during the lifetime of Cosmos 462

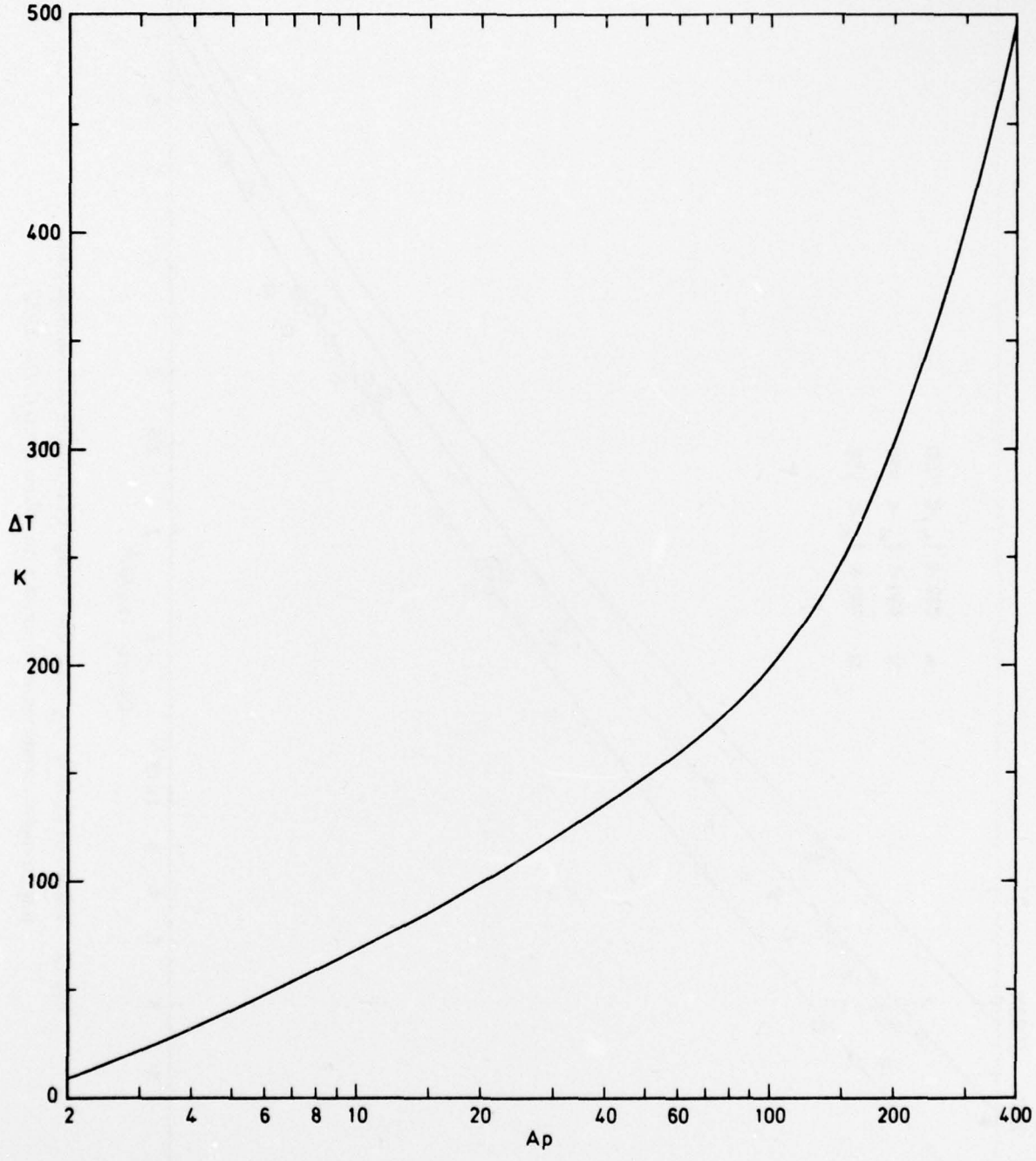

Fig 11 Variation of ΔT with Ap as specified by Jacchia in *CIRA 1972*

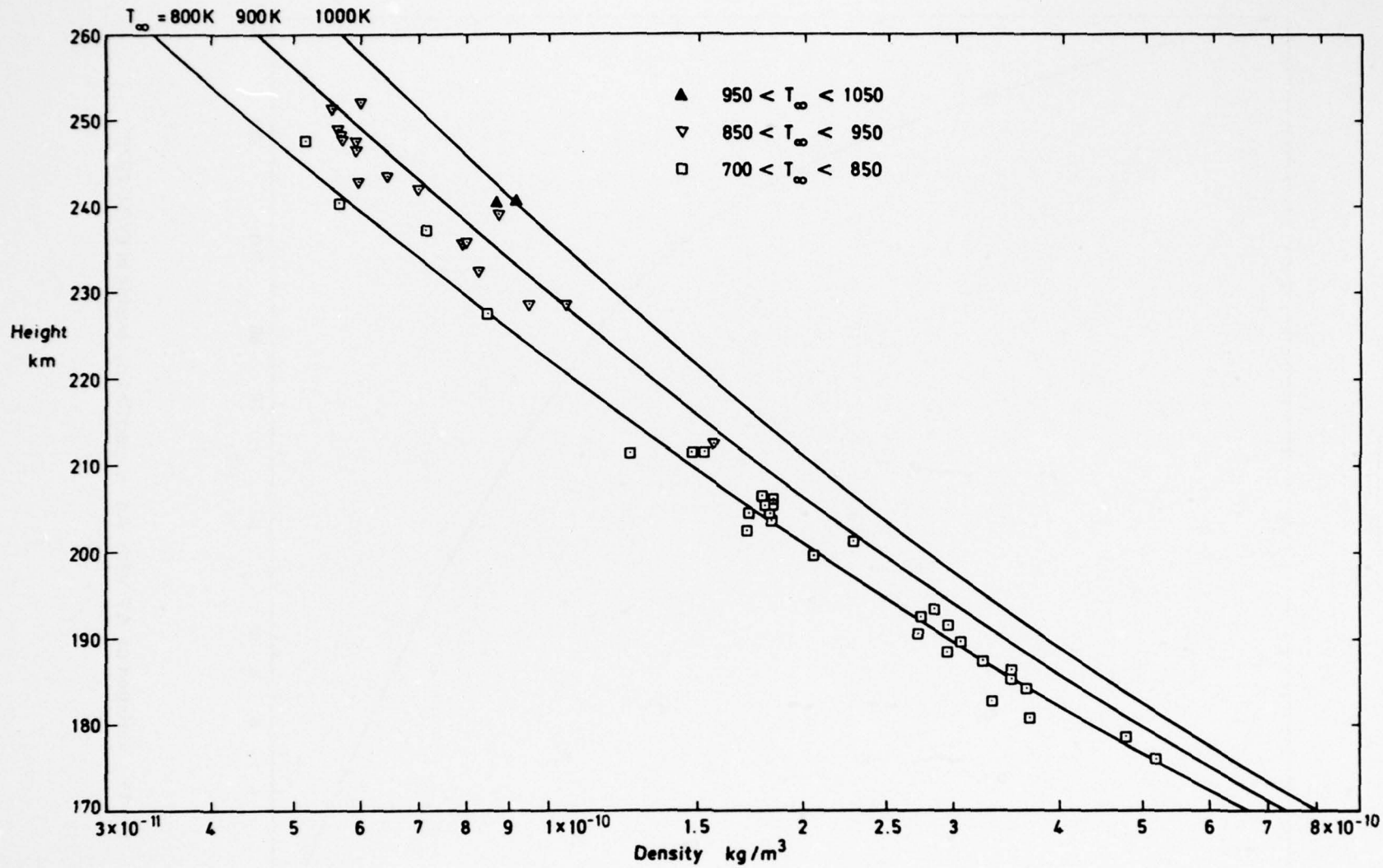

Fig 12 Values of density ρ_A near the average of both the semi-annual and day-to-night variations, compared with values from *CIRA 1972*

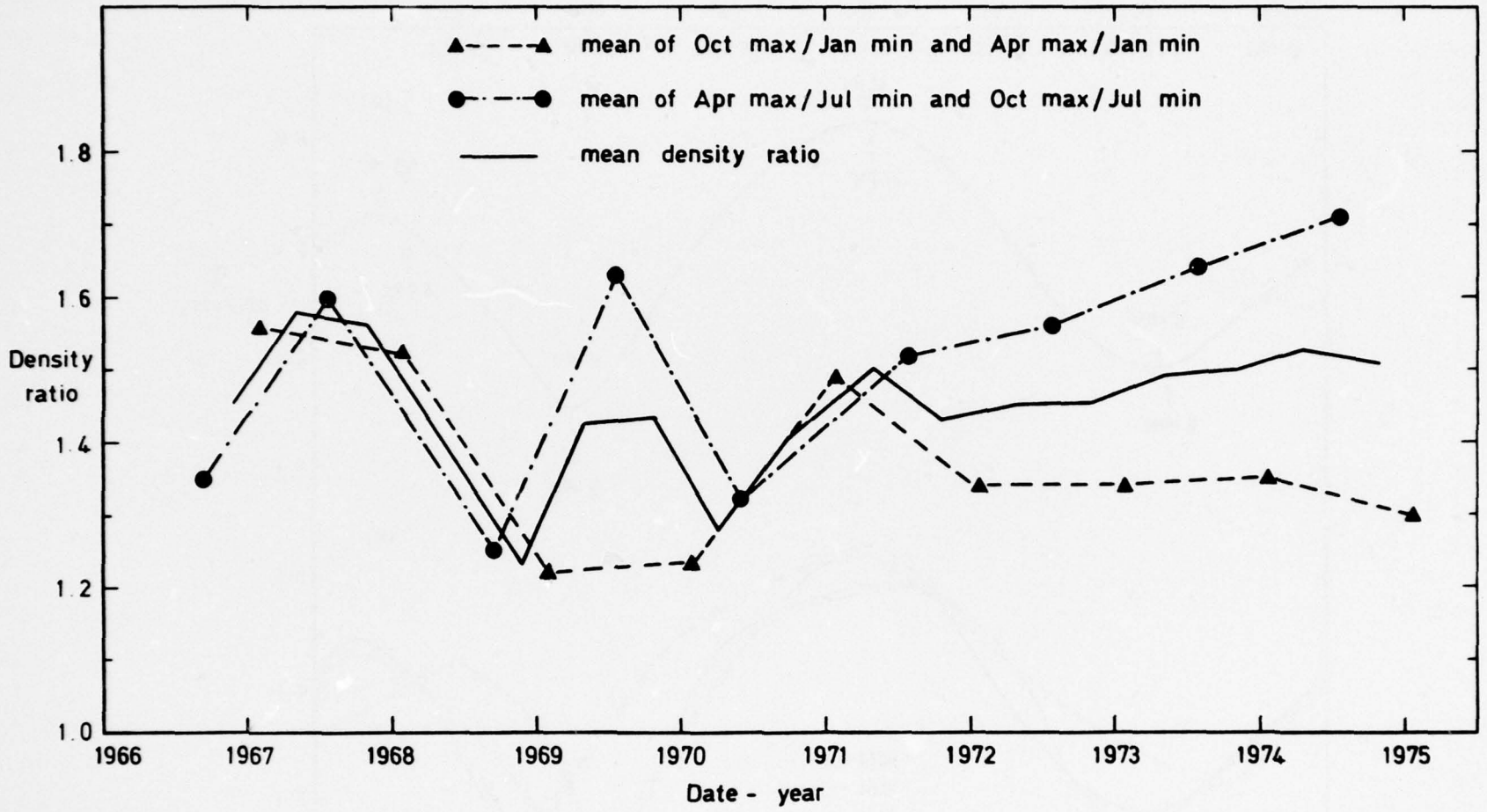

Fig 13 Maximum/minimum density ratio in the semi-annual variation, from 1966 to 1975

Fig 13

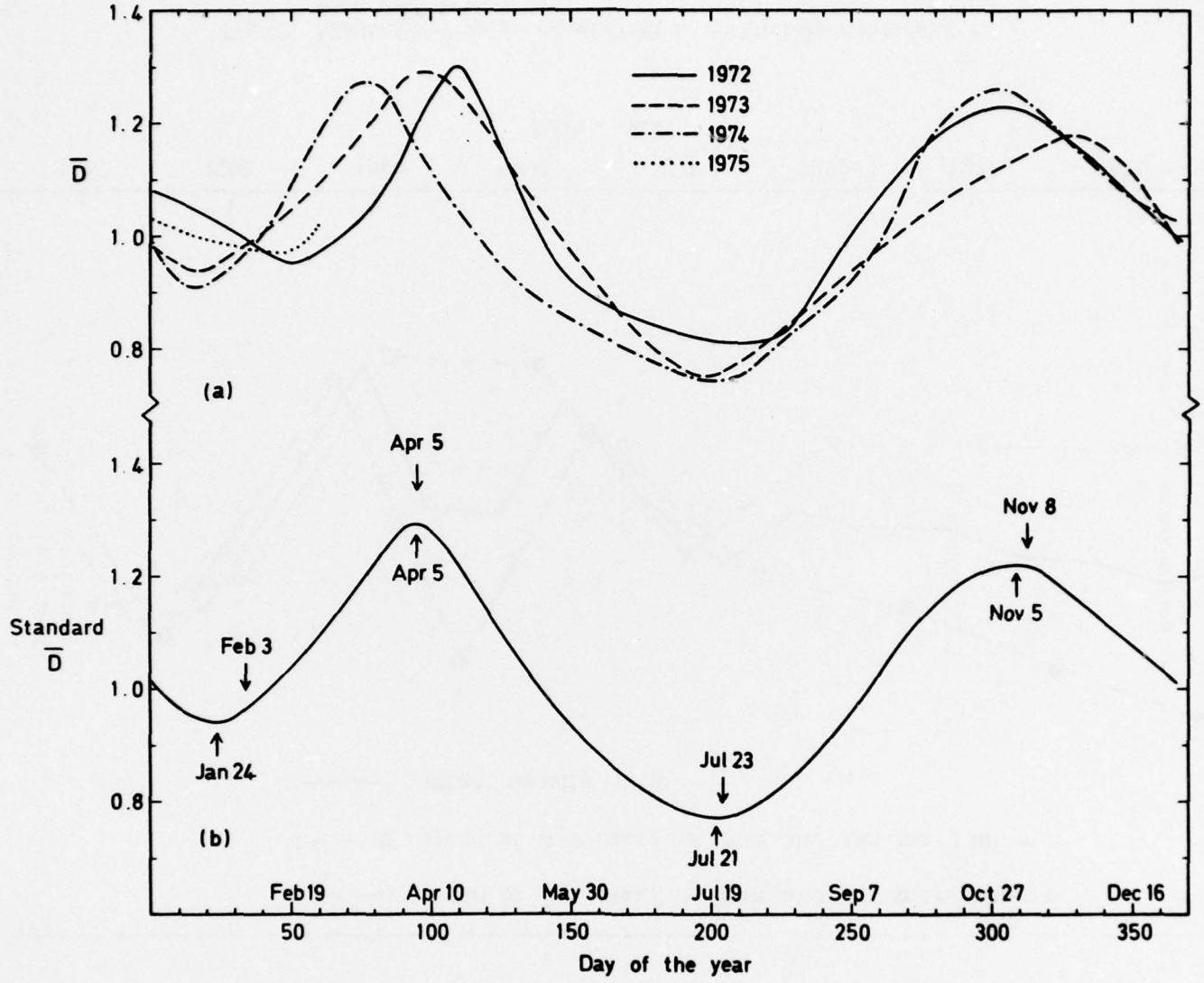

Fig 14 Variation of $\bar{D}$ and standard $\bar{D}$ during the year